Energy 368 (2026) 142820

Contents lists available at ScienceDirect

Energy

journal homepage: www.elsevier.com/locate/energy

Reducing the cost of solid sorbent direct air carbon capture by recovering waste heat from water electrolysis under Nordic conditions

Altti Meriläinen [a,*], Antti Kosonen [a], Peter Holtappels [b], Roland Dittmeyer [b], Pertti Kauranen [a], Jero Ahola [a]

[a] School of Energy Systems, Lappeenranta–Lahti University of Technology LUT, P.O. Box 20, FI-53851, Lappeenranta, Finland
[b] Institute for Micro Process Engineering, Karlsruhe Institute of Technology, Karlsruhe, Germany

ARTICLE INFO

Keywords:
Renewable hydrogen
Cost optimization
Power-to-X
Thermal energy storage (TES)
Heat pump
Levelized cost of DAC (LCODAC)

ABSTRACT

Reducing the atmospheric CO_2 concentration to a sustainable level requires large-scale carbon dioxide removal through direct air capture (DAC). DAC is a heat-intensive process, and waste heat recovery to supply its heat demand has substantial potential to reduce the levelized cost of DAC (LCODAC). This study determines the techno-economic potential of recovering low-temperature waste heat (70°C) from an off-grid electrolyzer plant for use in a solid-sorbent DAC plant requiring heat at 80°C–120°C for desorption. The waste heat recovery system, comprising heat pumps and a heat storage, and the DAC plant are dimensioned to minimize the LCODAC based on optimization at an hourly level, and a comparison with an electric-boiler-based heat supply is performed.

It was found that the 100 MW_e electrolyzer plant producing 6.3 kt/a of H_2 can provide heat for a DAC plant capturing up to 27 kt/a of CO_2 under Nordic conditions, where low ambient temperatures are beneficial for the solid DAC process, except for subzero temperatures. The LCODAC can be reduced by 21%–36% when a waste-heat-based heat supply is used instead of an electric boiler. Increasing the desorption temperature significantly reduces the LCODAC, even though the cost of heat supply increases due to the decreasing coefficient of performance of the heat pumps.

Waste-heat-based heat supply for DAC can benefit the electricity system, as it reduces the primary energy demand by about 62% and the peak electrical power by 57% compared with an electric boiler.

1. Introduction

Limiting the rise in global average temperature and its associated implications requires substantial direct greenhouse gas (GHG) emission reductions, as well as the removal of residual and already emitted GHGs from the atmosphere to reach net negative GHG emissions [1]. Roughly 65% of global GHG emissions are CO_2 emissions from the combustion of fossil fuels, either directly for energy generation or in industrial processes [1], and therefore, it is of primary importance to phase out fossil fuels. Direct electrification using renewable electricity is considered the most cost-effective method for replacing fossil fuels in energy generation and industrial processes, thereby directly decarbonizing these applications. For applications that are challenging to electrify directly, indirect electrification through power-to-hydrogen (H_2 used in, e.g., steelmaking and ammonia production) and power-to-hydrocarbons (such as production of fuels and materials derived from synthetic hydrocarbons) based on renewable electricity is considered the most promising approach [2]. The production of synthetic hydrocarbons requires CO_2 as a raw material, and the concept is based on a circular CO_2 economy, where CO_2 is captured from sustainable sources or unavoidable emissions, such as ambient air (direct air capture (DAC)) or point sources associated with biomass combustion, waste incineration, and cement production [3]. The concept is often referred to as carbon capture and utilization (CCU), in which CO_2 is captured and further processed into a product. In practice, CCU enables temporary carbon storage and carbon cycle, thereby directly reducing the use of fossil fuels [4], whereas permanent storage of the captured CO_2 through carbon capture and storage (CCS) prevents it from returning to the atmosphere [5]. Applied to fossil point sources, CCS avoids emissions that would otherwise occur, whereas net removal of CO_2 from the atmosphere requires permanent storage of atmospheric or biogenic CO_2, that is, through direct air carbon capture and storage (DACCS) or bioenergy with carbon capture and storage (BECCS), provided that no simultaneous CO_2 release to the atmosphere occurs [1].

* Corresponding author.
E-mail address: altti.merilainen@lut.fi (A. Meriläinen).

https://doi.org/10.1016/j.energy.2026.142820
Received 2 July 2026; Received in revised form 11 October 2026; Accepted 17 October 2026
Available online 7 November 2026
0360-5442/© 2026 The Authors. Published by Elsevier Ltd. This is an open access article under the CC BY license (http://creativecommons.org/licenses/by/4.0/).

Acronyms

AEMWE	Anion exchange membrane water electrolyzer
AWE	Alkaline water electrolyzer
BECCS	Bioenergy with carbon capture and storage
BECCU	Bioenergy with carbon capture and utilization
BESS	Battery energy storage system
CAPEX	Capital expenditure
CCS	Carbon capture and storage
CCU	Carbon capture and utilization
CDR	Carbon dioxide removal
COP	Coefficient of performance
DAC	Direct air capture
DACCS	Direct air carbon capture and storage
DACCU	Direct air carbon capture and utilization
EB	Electric boiler
EU	European Union
FOAK	First-of-a-kind
GHG	Greenhouse gas
HP	Heat pump
LCOCDR	Levelized cost of CDR
LCODAC	Levelized cost of DAC
LCOH	Levelized cost of heat
$LCOH_2$	Levelized cost of hydrogen
NOAK	Nth-of-a-kind
OPEX	Operational expenditure
PEMWE	Proton exchange membrane water electrolyzer
PTES	Pit thermal energy storage
PV	Photovoltaic
SEC	Specific energy consumption
SOWE	Solid oxide water electrolyzer
TES	Thermal energy storage
TVSA	Temperature-vacuum swing adsorption
VAT	Value added tax
WH	Waste heat

List of symbols

A	Area
C	Cost
c	Specific heat capacity
E	Energy
h	Specific enthalpy
i	Time step
m	Mass
n	Lifetime in years
P	Power
Q	Heat transfer
r	Discount rate
ρ	Density
T	Temperature
t	Time in years
U	U-value (thermal transmittance)
V	Volume

List of subscripts

ads	Adsorption
bal	Balance
dem	Demand
des	Desorption
e	Electricity
gen	Generation
h	Heat
min	Minimum
p	Peak

It has been estimated that limiting the rise in global average temperature to 1°C–1.5°C above preindustrial levels by 2100 requires emissions from the global energy–industry system to reach net zero by 2045–2050 through direct and indirect (CCU) electrification and CCS. After that, net carbon dioxide removal (CDR) is necessary and should be in the range of 11–39 Gt_{CO_2}/a from the early 2060s through 2100 to actively reduce atmospheric CO_2 to a sustainable level [6]. CDR can be implemented through nature- and technology-based options, including afforestation and reforestation, soil carbon sequestration, biochar, enhanced weathering, ocean alkalinity enhancement, BECCS, and DACCS [1]. Nature-based options are currently the least expensive pathways, but their potential is constrained by land availability, competition for land for food production, and the limited permanence of stored carbon, whereas BECCS is limited by the sustainable supply of biomass. In general, the maximum global mitigation potential for most of these options is approximately between 0.5 and 11 Gt_{CO_2}/a, whereas the potential for DACCS is 5–40 Gt_{CO_2}/a. Therefore, achieving the required CDR requires massive investment in the technological development of DAC, which offers the greatest potential among individual CDR options. It should also be noted that the carbon capture methods essential for producing renewable hydrocarbons include, in practice, direct air carbon capture and utilization (DACCU), bioenergy with carbon capture and utilization (BECCU), and biomass pyrolysis, from which the captured carbon gas can be subsequently utilized in the synthesis process.

There are several technological approaches to DAC, such as electro-swing adsorption, ambient weathering carbon capture, solid DAC, and liquid DAC, the latter two of which are the most mature technologies [7,8]. Liquid DAC relies on alkaline gas washing, in which the regeneration temperature is about 900°C, currently supplied by combusting natural gas. Solid DAC, on the other hand, relies on solid adsorbents, typically using a temperature-vacuum swing adsorption (TVSA) process at regeneration temperatures of 80°C–120°C. In the TVSA process, thermal energy can be delivered to the adsorbent either indirectly via heat exchangers or directly by passing steam through it (known as steam-assisted TVSA) [9]; the latter increases sorbent productivity but also the specific energy consumption (SEC) and may degrade some amine-based adsorbents [10,11]. In both technologies, the thermal energy demand accounts for about 80% of the total energy consumption of the DAC process [12], and the thermal energy demand is reported to be 1.0–5.0 MWh_h/t_{CO_2} for solid DAC and 1.5–3.5 MWh_h/t_{CO_2} for liquid DAC [9]. The main advantage of solid DAC is its modularity and smaller plant scale compared with liquid DAC, which can facilitate rapid technological advancement [9]. Space availability and land use are further constraints on large-scale DACCS deployment [13]: solid DACCS requires at least about 40% less land

than liquid DACCS and about 1% of the land required for BECCS over an 80-year time horizon [14]. The modularity and smaller plant scale of solid DAC also allow application in, for example, building ventilation systems, benefiting from existing infrastructure and increased CO_2 concentrations [15].

Climeworks, a pioneer in solid DAC, estimated in 2019 that the cost of CO_2 capture would be in the range of 500–600 $/t_{CO_2}$ (about 430–520 €/t_{CO_2}); however, for its first large-scale DACCS plant in Iceland, Orca (4 kt_{CO_2}/a), it quoted a carbon offset price of 1000 €/t_{CO_2} in 2021 [16]; this is a commercial offset price that covers capture, possible transport, and storage and includes a margin, and it is therefore not directly comparable with a modeled cost of capture. For liquid DAC, Carbon Engineering estimated a levelized cost of DAC (LCODAC) of 94–232 $/$t_{CO_2}$ (about 80–200 €/t_{CO_2}) for a 1 Mt_{CO_2}/a plant in 2018 [17], but its first large-scale plant is only now being built [18], and thus, a similar upward revision is likely. According to Herzog et al. [19], several recent modeling studies use a cost of capture in the range of 100–200 $/$t_{CO_2}$ (about 85–175 €/t_{CO_2}), while carbon removal credits are sold at 1500 $/$t_{CO_2}$ (about 1300 €/t_{CO_2}). They emphasize that unavoidable engineering challenges make such estimates somewhat unrealistic, and the cost of CO_2 storage is often ignored in DAC studies. This also means that terms related to the cost of CO_2 capture may be used in potentially misleading ways. In this study, the LCODAC covers the capture step and its energy supply, that is, the cost of atmospheric CO_2 as a raw material, whereas the levelized cost of CDR (LCOCDR) covers the entire chain from capture to permanent storage, including transport, storage, and the associated emissions, and thus represents the cost of net permanent carbon removal. Sievert et al. [20] introduced a new method to project current and future costs of DACCS and estimated that the LCOCDR of first-of-a-kind (FOAK) DACCS for liquid and solid DAC would be in the range of 521–894 $/$t_{CO_2}$ (about 450–775 €/t_{CO_2}) and 1180–1392 $/$t_{CO_2}$ (about 1020–1205 €/t_{CO_2}), respectively. At 1 Gt_{CO_2}/a cumulative capacity (nth-of-a-kind (NOAK) development phase), the LCOCDR would fall to 226–544 $/$t_{CO_2}$ (about 195–470 €/t_{CO_2}) and 281–579 $/$t_{CO_2}$ (about 245–500 €/t_{CO_2}).

The low regeneration temperature of solid DAC makes it suitable for industrial low-temperature waste heat sources [21]. The use of waste heat in DAC is of great interest, as heat supply constitutes a significant proportion of the total energy consumption of a DAC plant and the LCODAC. In addition, the use of waste heat or excess electricity can reduce the land use of DAC, as fewer new energy generation facilities need to be constructed. Wijesiri et al. [22] found that thermal energy accounts for about one-third of the LCODAC, and that free waste heat in the desorption process reduces the LCODAC by 42%, from 612 to 355 €/t_{CO_2}. Fasihi et al. [23] studied the techno-economics of DAC plants in Morocco using heat-pump-based heat supply and reported the LCODAC for solid DAC to be 222 €/t_{CO_2} in 2020; they estimated that the cost would decrease to 54 €/t_{CO_2} in 2050. The use of free waste heat was found to reduce the above-mentioned LCODAC by 40%–57%. Terlouw et al. [13] studied the potential and techno-economic performance of solid-sorbent-based DACCS in 27 European countries, also analyzing the potential for waste-heat-based heat supply. They calculated the LCOCDR across the whole supply chain from DAC to permanent storage, also considering the cost of gray emissions (emissions from power generation for DAC). They found that the average LCOCDR decreases from 830 to 650 €/t_{CO_2} when considering heat supply based on free waste heat instead of a high-temperature heat pump. Their results also show high variability in the LCOCDR among the European countries under analysis, mainly due to variations in the GHG intensity of the electricity grid, which drive gray emissions, and different capital expenditure (CAPEX) for DAC under different market and climate conditions. Common to these studies is that waste heat is treated as a free and continuously available resource at a temperature that matches the desorption process, and that the equipment needed to make the waste heat usable is not costed out. In addition, the characteristics of the heat sources used by the heat pumps in these studies remain largely unclear, with assumed coefficient of performance (COP) values of approximately 2–3.5 at a desorption temperature of 100°C [13,20,23]. COP values of 2 and 3 would allow temperature lifts of approximately 75°C–85°C and 40°C–55°C, respectively [24,25]. Therefore, ambient air cannot serve as the heat source at a COP close to 3 and at a heat demand temperature of 100°C; a higher-temperature source, such as waste heat, is required. Moreover, the waste heat considered in these studies originates from industrial processes, whereas water electrolysis is expected to become a major source of low-temperature waste heat and has thus far been investigated primarily as a heat source for district heating [26,27]. Its potential to supply DAC, which is also the source of the CO_2 required by power-to-hydrocarbons synthesis [3,28], has not been assessed.

The performance of solid DAC benefits from a colder (adsorption temperature of about 10°C) and drier (ambient air relative humidity of about 10%–20%) environment [29,30]. In liquid DAC systems, the behavior is opposite, as warm and humid conditions improve the performance [31,32]. Cold conditions are thus advantageous for solid DAC, but only down to a limit, as the feasible adsorption temperature is generally limited to 0°C–30°C, because at subzero temperatures the freezing of condensed water may cause operational issues, and adsorption temperatures exceeding 30°C impose considerable constraints on performance [11,29]. For example, Climeworks' Orca plant in Iceland has encountered unexpected problems, including freezing, leading to reduced operating hours [9]. Under Nordic conditions, the 0°C limit is decisive, as it shuts down the plant for a large part of the winter; enabling operation under subzero conditions would therefore considerably increase the operating hours. Previous studies have set the minimum adsorption temperature anywhere between 5°C and −15°C [13,29,30,33,34] without demonstrating the economic value of the operating hours thereby gained or quantifying the possible additional cost that subzero operation would incur.

Climatic conditions and the availability of low-cost energy are the main factors determining where DAC can be deployed most economically [35,36]. Jajjawi et al. [30] studied the techno-economic feasibility of solid DAC in four regions (U.S., Germany, Nigeria, and Norway) and found that the minimum LCODAC can be achieved in Germany, whereas Nigeria, with its hot and humid climate, represents the highest LCODAC if the investment and energy costs are assumed to be the same between the regions. They also analyzed a scenario in which the specific investment cost of the DAC plant depends on the local climate and the energy supply is based on local solar photovoltaic (PV) power, batteries, an electric heater, and a heat pump, resulting in the LCODAC being most affordable in the U.S. and second most affordable in Nigeria. Again, the heat pump was assumed to supply heat for desorption at 90°C with a constant COP of 2 in all locations.

To ensure cost-effective utilization of waste heat sources, it is advantageous for the waste heat temperature to be as close as possible to the temperature required for the desorption of DAC, thus minimizing the need for supplemental temperature elevation, such as by a heat pump. However, it has been estimated that most of the waste heat available globally is at low temperature (<100°C) [37,38], resulting in limited potential for direct use in applications requiring heat at, for example, 100°C. It would be possible to operate desorption in DAC at lower temperatures, thus adapting the process to the available waste heat temperature. In practice, lowering the desorption temperature reduces the performance of a solid DAC system, whereas a higher desorption temperature is highly beneficial from the perspective of CO_2 productivity and SEC [11]. Therefore, the challenge may be that the performance loss of DAC exceeds the achieved cost benefit. Ge et al. [34] demonstrated that heat-pump-assisted waste heat recovery even at 20°C reduces the SEC of solid DAC by at least 40% compared with an electric boiler, and reported a 61% lower net operational cost, although only at a single operating point (waste heat at 60°C, desorption at 100°C) and with the capital expenditure, maintenance, and labor excluded. Therefore, limited information is available on how the economic profitability of waste heat integration into solid DAC

varies as a function of desorption temperature, as only its technical effect has been studied.

The objective of this techno-economic analysis is to determine how much CO_2 can be captured, and at what cost, by recovering the waste heat of a 100 MW_e off-grid alkaline water electrolyzer (AWE) plant for use in a TVSA-based DAC plant. A waste heat recovery system between the AWE plant and the DAC plant is cost-optimally designed to minimize the LCODAC based on optimization at an hourly level. Power generation for the off-grid AWE plant is based on local solar PV and wind power, resulting in variable waste heat output at 70°C. Therefore, the waste heat recovery system comprises heat pumps and a thermal energy storage (TES), which are employed to supply waste heat to the desorption process of the DAC at 80°C–120°C. To determine the profitability of waste heat integration into DAC, a comparison is made with a conventional scenario using an electric-boiler-based heat supply. The work analyzes whether lowering the desorption temperature is techno-economically profitable, as the profitability of waste heat recovery decreases with an increasing temperature lift due to the decrease in the COP of the heat pump. In addition, this study aims to determine the economic margin available for the additional costs of operating the DAC at subzero temperatures to increase its operating hours under Nordic conditions. Such operation remains an open question, as it may introduce costs related to freeze prevention, material durability, and increased maintenance, for which the literature provides limited quantitative basis. The subzero case is therefore treated in this work as an idealized scenario in which continuous operation down to −10°C is assumed and no freezing-related downtime or additional cost is included.

To the best of the authors' knowledge, the identified novelty and the corresponding research gaps are as follows:

- Techno-economic potential of recovering waste heat from water electrolysis into solid DAC is determined, as the existing literature on this topic remains limited.
- The cost of variable waste heat integration is analyzed and optimized by dimensioning the heat pumps and the TES to minimize the LCODAC.
- The impact of desorption temperature on the techno-economic profitability of waste heat recovery and the DAC plant is analyzed.
- Electrical energy and power demand of the waste heat integration are quantified and compared with electric-boiler-based heat supply. While studies have examined the electricity system impacts of solid DAC under electricity-based heat supply configurations [39], such system-level implications have not been assessed for waste-heat-based integration concepts.
- The economic margin available for the additional costs of subzero operation is quantified by comparing minimum adsorption temperatures of 0°C and −10°C.

It is worth noting that the aim of this work is not to model the subsystems or their integration with process-level fidelity, but rather to use simplified models to understand, at the system level, the techno-economic feasibility of waste heat recovery from an off-grid alkaline water electrolyzer plant into a TVSA-based DAC plant. Simplified system-level modeling provides a rapid method for examining interactions within sector-coupled systems. Focusing on a single subsystem does not reveal how it affects the surrounding energy system or how the surrounding energy system affects its operation. These interactions are often overlooked when individual subsystems are modeled in excessive detail, as the resulting computational requirements can quickly become prohibitive. The work can be viewed as the first stage of an investment process, a feasibility study, intended to determine whether the concept is economically attractive and therefore warrants further, more detailed process-level investigation.

2. Methodology

The methodology is primarily based on the authors' previous studies, which investigated waste heat recovery from a 100 MW_e off-grid AWE plant for use in district heating [40,41]. The off-grid AWE plant designed and optimized to supply baseload H_2 at 12 kg/min is based on local wind and solar PV power generation supported by a battery energy storage system (BESS) and a hydrogen storage [42]. AWE is used because it is considered the most mature electrolyzer technology for large-scale renewable hydrogen production [43] and because the off-grid plant providing the waste heat profile was previously cost-optimized for this technology [42]. A proton exchange membrane water electrolyzer (PEMWE) and an anion exchange membrane water electrolyzer (AEMWE) would reject heat at comparable temperatures [44], and the results are therefore transferable also to these technologies, as the analysis is governed by the temperature level and the generation profile of the available waste heat rather than by the electrolysis technology itself. The low-temperature AWE, PEMWE, and AEMWE technologies require process cooling, whereas the high-temperature solid oxide water electrolyzer (SOWE) technology requires heat input in the form of steam at 700°C–900°C. Therefore, SOWE is usually treated as a heat sink for high-temperature industrial waste heat, while recovering waste heat from the SOWE process is beneficial for preheating the process feedwater [45]. In addition, SOWE requires a constant operating environment, making it challenging to couple with variable power generation. The characteristics of the 100 MW_e off-grid AWE plant are based on cost optimization at a 15-minute resolution using a 30-year lifetime for the plant, cost assumptions for the year 2025 with a 5% discount rate, and measured power generation data from 2021 for existing wind and solar PV installations in southeastern Finland. Table 1 provides the key information of the AWE plant. The optimization of the AWE plant considered age-related degradation of the system components, resulting in an increase in the waste heat of the electrolyzer over time. Therefore, this work uses the waste heat generation profile from the first year of operation, which has the lowest waste heat availability of the plant lifetime. Dimensioning the waste heat recovery system according to a later year would leave it operating below its rated capacity for most of the plant lifetime, which is not cost optimal, whereas dimensioning it according to the first year ensures that at least the design value of the waste heat is available throughout the plant lifetime. The surplus electricity generation refers to curtailed wind and solar PV power generation that is not used to power the AWE, because the whole AWE plant is dimensioned from the techno-economic perspective to minimize the levelized cost of hydrogen, which results in overdimensioned solar PV and wind power generation capacity [42,46,47]. This curtailed electricity can be considered available for use if it can be used locally, and in this case, it can be supplied to the DAC or heat pumps. In addition, more detailed information about the AWE plant, such as duration curves for waste heat and surplus electricity generation, can be found in [41].

The main difference between the current and previous studies by the authors [40,41] lies in the heat sink and its characteristics when the district heating system is replaced by the DAC plant. The structure of the waste heat recovery system is illustrated in Fig. 1(a), and it consists of two main components: heat pumps and a pit thermal energy storage (PTES). There are two heat pumps in the system: a heat pump for PTES (HP_{PTES}) and a heat pump for direct waste heat consumption (HP_{direct}). The latter is used to boost the temperature of the waste heat, which is directly consumed in the desorption process in the DAC plant. Because the heat generation and demand are highly variable, the PTES is used to store part of the waste heat generated. The PTES is a large-scale sensible heat storage in which water contained in an insulated and lined excavated pit serves as the storage medium. Its operating principle, modeling, and specific investment cost are described in Appendix B. The task of the HP_{PTES} is to charge and discharge the PTES, where the temperature varies based on the state of charge of the PTES. However,

Table 1
Cost-optimized component capacities (or maximum power during the first year of operation) of the baseload H_2 off-grid AWE plant and the related energy outputs during the first year of operation [42]. The conversion from energy to the mass of hydrogen is performed using the higher heating value of hydrogen. The BESS is employed to increase the full load hours of the electrolyzer. The waste heat is assumed to be available at 70°C on the secondary side of the electrolyzer cooling circuit.

Component	Capacity or P_{max}	First-year energy output
Wind power	121 MW_e	362.2 GWh_e
Solar PV	68 MW_p	61.0 GWh_e
BESS	27 MWh_e	8.5 GWh_e
AWE	100 MW_e	277.4 GWh_{H_2} (7.0 kt_{H_2})
Hydrogen storage	570 t_{H_2}	6.3 kt_{H_2}
AWE waste heat	24.0 MW_h	85.7 GWh_h
Surplus electricity	76.2 MW_e	25.5 GWh_e

the need for heat pumps depends on the temperature levels of the waste heat supply, the heat demand of the DAC, and the PTES. The use of two heat pumps can be beneficial from the perspective of energy efficiency, as the HP_{direct} can operate with a constant temperature lift, transferring heat from the constant temperature waste heat source to the desorption process of the DAC plant, which is assumed to operate at constant temperature. The HP_{PTES}, on the other hand, extracts heat from the PTES, whose temperature varies according to the state of charge, thereby reducing the COP compared with the HP_{direct} when the PTES temperature is lower than the waste heat temperature. The general concept is that the water electrolysis operates off-grid, using only local power generation, thereby avoiding any additional load on the electricity system. Nonetheless, for safety reasons, the plant is expected to require some level of electricity connection, which could, in principle, also provide electricity for the waste heat recovery and the DAC plant and allow the export of surplus electricity. The electricity supply for the heat pumps and the DAC plant is primarily met by local surplus electricity generation; when insufficient, electricity is imported from the grid. Export of electrical energy and the resulting income are not considered to avoid optimism. In addition, the techno-economic indicators of waste-heat-based heat supply for the DAC are compared with those of electric-boiler-based heat supply (Fig. 1(b)), which can be considered the conventional method for supplying the thermal energy demand of the DAC.

2.1. Model of the direct air capture plant

The model for a closed-inlet TVSA DAC plant (without steam) is based on a study by Luukkonen et al. [11], where the impact of different model and operating parameters on the performance of a solid DAC was studied using a dynamic fixed-bed model validated with experimental data. They found that optimizing the length of the adsorption step is particularly important for improving the performance of the DAC process; this was shown by comparing three different cut-off criteria, in which adsorption is terminated when the CO_2 loading of the adsorbent reaches 60%, 75%, or 90% of the equilibrium adsorption capacity. The comparison indicates that the adsorption cut-off criterion between 60% and 75% prevents adsorption from becoming inefficient due to excessive duration and yields the highest CO_2 productivity even though it increases the SEC of the process. Therefore, the selection of the 60% criterion is warranted in the present study, as it also demonstrates better performance than the 75% criterion when the adsorption temperature is below 10°C, as is typical under Nordic conditions. The results reported in [11] cover SEC and CO_2 productivity at different operating points, for which characteristic curves are fitted to provide a simplified approach for modeling the DAC process under varying operating conditions. These characteristic curves serve as the basis for the electrical and thermal energy demand as well as the CO_2 productivity of the DAC plant in the present study.

The characteristic curves are shown in Fig. 2. There are three operating parameters that are affected only by the properties of the supplied air: CO_2 concentration, relative humidity, and temperature. Luukkonen et al. [11] investigated the effect of adsorption temperature down to a minimum of 0°C based on the premise that adsorption temperatures below 0°C may cause operational issues due to moisture freezing. The base assumption in the present study is that the DAC plant cannot be operated at temperatures below 0°C, which will significantly reduce the operating hours of any DAC plant under Nordic conditions. However, a sensitivity analysis is performed with a minimum adsorption temperature of −10°C to evaluate the potential economic benefit if the same DAC plant could be operated in subzero temperatures. Because the characteristic curves provided by Luukkonen et al. [11] extend only down to 0°C, the curves are extrapolated for adsorption temperatures between 0°C and −10°C (Fig. 2(c)). Subzero adsorption has also been considered in the recent literature. Jajjawi et al. [30] modeled adsorption temperatures down to −10°C, and Luukkonen and Elfving [48] subsequently extended the model underlying the characteristic curves used here to the same limit, whereas Sendi et al. [29] permitted operation down to −15°C, following the specification sheet of the first-generation Climeworks unit, but assumed the performance below 1°C to equal that at 1°C. The extrapolated characteristic curves exhibit similar behavior to those of Jajjawi et al. [30], whose model is validated down to −10°C, and the extrapolation is therefore considered adequate for representing the DAC plant at subzero temperatures. In addition, a parameter that is essential from the perspective of the COP of heat pumps is the desorption temperature, whose impact on the techno-economics of waste heat integration into DAC is evaluated in this paper. It is noteworthy that the SEC decreases as the desorption temperature increases. While increasing the desorption temperature raises the absolute energy demand of the DAC, the CO_2 productivity increases by a larger relative amount, resulting in a lower SEC (see the supplementary material of [11]).

The SEC and CO_2 productivity values reported by Luukkonen et al. [11] are based on the operation of a single DAC unit, for which the duration of a single operating cycle (adsorption, blowdown, desorption, and cooling) varies as a function of operating parameters. However, a large-scale DAC plant can consist of tens or even hundreds of DAC units depending on its size, in which case the cycles of an individual unit can be hardly distinguishable from the collective operation. In this work, it is assumed that paralleling the units and interleaving the operation phases among them result in a steady demand for electricity and heat, as well as continuous CO_2 capture, when considering operation at an hourly resolution. Therefore, the daily CO_2 productivity reported in [11] is divided by 24 to obtain an hourly profile. A similar cycling sequence of multiple adsorbent beds has been described at the second level in [49,50], where temperature (vacuum) swing adsorption for post-combustion carbon capture was analyzed at the process level. Ultimately, the scheduling between DAC modules is a plant-level design and operational issue, the importance of which has been emphasized to avoid unnecessary peak power demand that increases capital and operational expenditures and to enable efficient integration with variable renewable energy sources [51].

In addition, the cooling energy demand of the DAC plant is ignored as it is assumed to be insignificant compared with the thermal energy demand. For instance, Rezo et al. [52] showed that the cost of cooling constitutes only a small share of net carbon capture costs, on the order of a few percent under summer conditions in Germany. In the present study, the temperature of the adsorbent is assumed to be cooled below the oxidative degradation threshold before pressurization with ambient air by transferring heat from the heating/cooling circuit to the ambient air using an air cooler, similarly to the approach in [53]. In this case, the cooling energy demand is solely due to the circulation pumps and fans (electricity). It is also important to note that because cooling is assumed to rely solely on electricity, neglecting it does not affect the

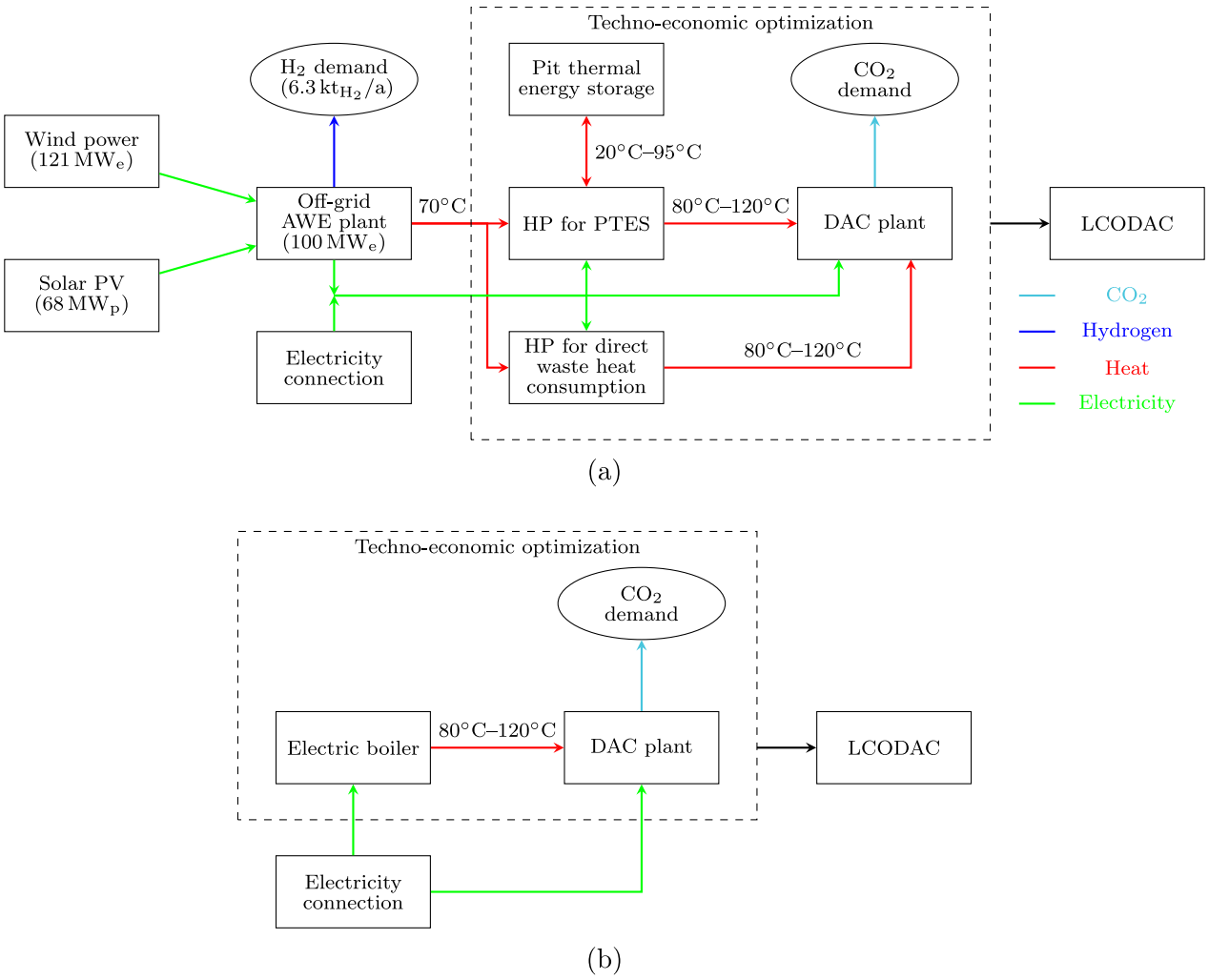


Fig. 1. (a) Simplified description of the waste heat recovery system describing the main components and the direction of energy flows. The electricity supply for the waste heat recovery system includes the surplus electricity from the AWE plant and the electricity drawn from the electricity connection. Heat pumps are used when a temperature lift is required; otherwise, they are not employed. (b) Reference case in which thermal energy for the DAC is supplied by an electric boiler. The scope of the study is enclosed within the dashed line in both subfigures.

conclusions of this study, which are based on the supply of thermal energy to the DAC process.

As the off-grid AWE plant is based on power generation data from southeastern Finland, the weather data for the DAC plant are obtained from the same area. Ambient temperature and relative humidity for the year 2021 were measured by the Finnish Meteorological Institute and are shown in Fig. 3. In the Nordic climate, temperature and humidity fluctuate substantially throughout the year, creating diverse but challenging conditions for DAC, especially in winter. CO_2 concentration in the ambient air is assumed to be constant at 400 ppm.

2.2. System simulation and cost optimization

The system modeling and simulation procedure between the waste heat supply (AWE plant) and the heat demand (DAC plant) follows the methodology described in our previous study [41]. Fig. 4 shows the flowchart of the simulation process, including the main equations used in the simulation and decision-making related to the control of the system. In practice, the simulation process is straightforward: decisions about the operation of the heat pumps are based on comparing the temperatures of the waste heat, the PTES, and the desorption process of the DAC plant. The heat power balance after direct waste heat consumption and the availability of waste heat determine whether the PTES has to be discharged to the desorption process or whether it can be charged with the waste heat. Modeling of the heat pumps and the PTES is described in Appendices A and B, respectively.

The target of the cost optimization is to dimension the waste heat recovery system (heat pumps and the PTES) and the DAC plant to minimize the LCODAC. The LCODAC is determined as follows (adapted from [23,29]):

$$\mathrm{LCODAC} = \frac{\mathrm{CAPEX} + \sum_{t=1}^{n} \frac{\mathrm{OPEX}_t + C_{\mathrm{sorbent,replacement},t}}{(1+r)^t}}{\sum_{t=1}^{n} \frac{m_{\mathrm{CO_2,captured},t}}{(1+r)^t}}, \quad (1)$$

where CAPEX is the total CAPEX, OPEX_t is the total annual operational expenditure (OPEX), $C_{\mathrm{sorbent,replacement},t}$ is the sorbent replacement cost, $m_{\mathrm{CO_2,captured},t}$ is the annual CO_2 captured, r is the discount rate, t is the individual year of lifetime of the system, and n is the lifetime of the system. CAPEX and OPEX consist of the following components: $\mathrm{HP_{direct}}$, $\mathrm{HP_{PTES}}$, PTES, DAC plant, and electricity purchase (OPEX only). The optimization variables and their boundaries are shown in Table 2. The capacity of the DAC plant is determined by the sorbent mass, which is also used to derive the hourly electrical and thermal energy demand as well as the hourly CO_2 capture based on the characteristic curves of the DAC (Fig. 2) and the ambient temperature and humidity (Fig. 3). The cost optimization is performed with the particle swarm optimization algorithm of MATLAB. As the algorithm is stochastic,

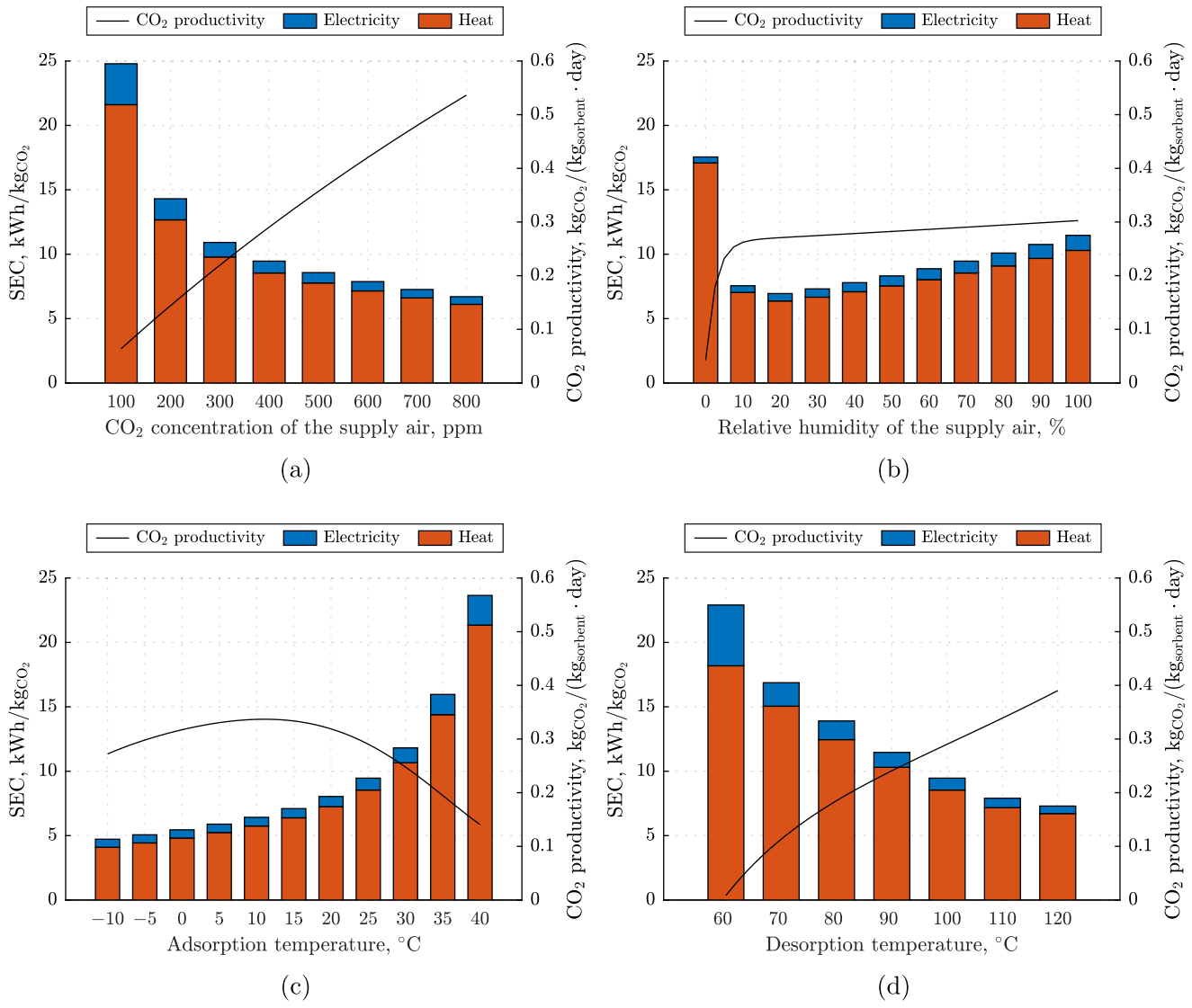


Fig. 2. Characteristic curves for the TVSA-based DAC model [11]. The curves illustrate the base case (CO_2 concentration 400 ppm, relative humidity 70%, adsorption temperature 25°C, and desorption temperature 100°C) and the change from this base case.

Table 2
Optimization variables and their boundaries. The electric boiler capacity is optimized only in the reference case (see Fig. 1).

Variable	Min	Max
Sorbent mass in the DAC, t	0	500
PTES volume, m^3	0	10×10^6
PTES temperature at the beginning of the year, °C	20	95
HP_{direct}, MW_h	0	50
HP_{PTES}, MW_h	0	50
Electric boiler, MW_h	0	50

repeated optimizations may yield slightly different results. This affects mainly the cost-optimized capacities and, to a lesser extent, the annual CO_2 capture, whereas the LCODAC remains practically unchanged (Appendix F).

Two constraints are set for the waste heat recovery system in the cost optimization. The temperature difference of the PTES between the first and last time step of the year must be in the range of 0°C–0.5°C (in other words, the energy content must be approximately the same):

$$0 \leq T_{\text{PTES,end}} - T_{\text{PTES,0}} \leq 0.5, \tag{2}$$

where T_{PTES} is the temperature of the PTES at the beginning (0) or at the end (end) of the simulation period. In addition, to achieve a maximum yet realistic waste heat utilization rate, at least 95% of the waste heat available from the off-grid AWE plant must be recovered (either directly or by charging the PTES):

$$E_{\text{WH,DirectUse}} + E_{\text{WH,ToPTES}} \geq E_{\text{WH}} \cdot \eta_{\text{recovery}}, \tag{3}$$

where $E_{\text{WH,DirectUse}}$ is the total waste heat energy that is directly consumed, $E_{\text{WH,ToPTES}}$ is the total waste heat energy that is used to charge the PTES, E_{WH} is the total available waste heat, and η_{recovery} is the recovery rate (95%). The recovery rate is set deliberately high, as the objective of this study is to determine how much CO_2 can be captured with the waste heat available from the 100 MW_e off-grid AWE plant. It is not 100%, because full recovery would require the waste heat recovery system to accommodate every hour of waste heat availability irrespective of the cost of doing so, which would no longer necessarily correspond to a cost-optimal design. The constraint is nevertheless what couples the capacity of the DAC plant to the AWE plant: it forces the waste heat recovery system and the DAC plant to be dimensioned according to the seasonal profile of the available waste heat rather than to a freely chosen CO_2 capture target, and the annual CO_2 capture is thus determined by the waste heat available.

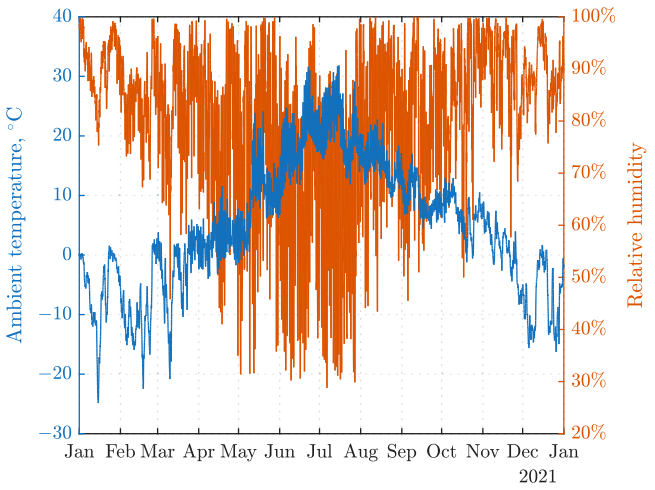


Fig. 3. Ambient temperature and relative humidity in Lappeenranta, south-eastern Finland.

Cost assumptions for the technologies are shown in Table 3. An effort has been made to formulate the techno-economic assumptions such that they correspond to current cost levels, that is, approximate FOAK conditions. It must be recognized, however, that there are significant uncertainties regarding the costs of DAC technology. For example, the cost of the sorbent presented in the literature is in the range of 0.2–80 $/kg [54]. A few studies have used a sorbent cost estimate of 30 €/kg or 30 $/kg, which is approximately 50% of the current laboratory-scale price [55,56]. A report by the National Academies [57] presented an adsorbent purchase cost of 50 $/kg (approximately 42 €/kg) for a generic solid sorbent DAC system under a medium-price scenario. In general, the sorbent is a major cost component of the CAPEX and life-cycle cost of solid DAC systems due to the cost and lifetime of the sorbent material. At the current cost level, the share of the initial sorbent in the total CAPEX of a solid DAC plant is estimated to be approximately between 70% and 90% for annual capture capacities of about 90 kt_{CO_2}/a and 1 Mt_{CO_2}/a, respectively [55,57]. It should be noted that in the aforementioned studies, the CAPEX distribution is presented for a specific sorbent cost (30–50 €/kg), and it may differ if the sorbent cost or the scale of the DAC plant changes significantly, thereby altering the share of other equipment in the DAC plant. Nevertheless, as a best available estimate, the capacity of the DAC plant in this work is determined by the sorbent mass; therefore, the CAPEX of the DAC plant is tied to the sorbent mass, assuming that the sorbent accounts for 80% of the CAPEX and other equipment for 20%. According to [20], a realistic assumption for the sorbent lifetime is 1–3 years; in addition, [55,56] assumed a lifetime of 2 years for existing sorbents (Lewatit VP-OC-1065 and MIL-101). Consequently, replacement of the sorbent material represents a variable OPEX for the DAC plant. Beyond this variable cost, a fixed OPEX is applied for the total DAC plant investment. While a fixed OPEX of 4% is a common estimate in the literature [23,56], the value is rounded to 5% in the present study to account for uncertainties in technology costs. The other components (heat pump, electric boiler, and PTES) represent mature and widely deployed technologies, providing substantially more reliable cost estimates. The assumption is that the DAC investment does not include an investment in the heat supply of the DAC, but that all costs related to heat supply consist of either the waste heat recovery system or the electric boiler.

To assess the effect of the investment cost of the DAC on the LCO-DAC, a sensitivity analysis is performed using a sorbent cost of 20 €/kg, assuming that the sorbent still accounts for 80% of the plant's total CAPEX. Considering the economic assumptions, a sensitivity analysis is also conducted by varying the discount rate, because it typically has a considerable impact on the economy of capital-intensive renewable energy technologies (see Appendix D). Appendix D also presents a sensitivity analysis of sorbent lifetime (1–3 a), as this parameter is subject to considerable uncertainty. This analysis is essential because the selected adsorption cut-off criterion of 60% subjects the sorbent to more cycles than higher cut-off criteria and may therefore accelerate sorbent degradation. In addition, the impact of desorption temperature on the techno-economics of the waste heat recovery system is assessed using desorption temperatures of 80°C, 100°C, and 120°C. The reference scenario with electric-boiler-based heat supply (Fig. 1(b)) is analyzed for the 100°C case only. A further parameter considered in the sensitivity analysis is the minimum adsorption temperature of the DAC, and the techno-economic performance of the DAC plant is evaluated using minimum adsorption temperatures of −10°C and 0°C, as described in Section 2.1. Finally, two additional comparisons are conducted at the desorption temperature of 100°C (Appendix F). First, the temperature of the waste heat is varied between 0°C and 120°C, while the hourly waste heat profile is kept unchanged, and the system is re-optimized for each temperature. This shows the effect of the temperature level of the waste heat alone. Second, an air-source heat pump without waste heat recovery is analyzed as an alternative to the electric boiler in order to obtain an indicative estimate of the benefit of the waste heat compared with ambient air as the heat source.

3. Results

The results are organized as follows: first, the technical performance of the DAC plant with different desorption temperatures and minimum adsorption temperature limits is presented. Second, the techno-economic indicators of the waste heat recovery and the CO_2 capture are described. Unless otherwise stated, the results presented in this section correspond to the base-case assumptions of Table 3, in particular a sorbent lifetime of 2 a and a discount rate of 6%.

3.1. Performance of the DAC plant

Fig. 5 illustrates the SEC and CO_2 productivity of the DAC plant on an annual and monthly basis. The SEC decreases significantly with an increasing desorption temperature, with values of 10.0–10.4 kWh/kg_{CO_2} at $T_{DAC,des}$ = 80°C and about 5.2–5.4 kWh/kg_{CO_2} at $T_{DAC,des}$ = 120°C. At the monthly level, the SEC is fairly uniform, except during the summer months (June–August), when it increases due to higher adsorption temperatures (see Figs. 2 and 3). About 90% of the SEC consists of heat consumption, which is a typical value for solid DAC systems. The CO_2 productivity increases substantially with the increase in desorption temperature and is more than doubled at $T_{DAC,des}$ = 120°C compared with $T_{DAC,des}$ = 80°C on an annual basis. The difference in the SEC between the scenarios of $T_{DAC,ads,min}$ = 0°C and $T_{DAC,ads,min}$ = −10°C is very small, but the CO_2 productivity increases by about 29% annually due to increased operating hours during the winter months (December–March). The operating hours increase by 31% from 5974 to 7825 h/a.

3.2. Techno-economic analysis of waste heat recovery

Cost-optimized capacities of the system are illustrated in Fig. 6. The total heat pump capacity consists mainly of the HP_{PTES}, meaning that almost all available waste heat is supplied to consumption through the PTES. Only a very small proportion of the available waste heat is directly consumed using the HP_{direct}. The reason is that the operating hours of the HP_{direct} are not sufficiently high, because the heat demand of the DAC plant is zero for a significant period in winter. HP_{PTES} is needed in any case to discharge and/or charge the PTES, and the practical solution would most likely consist only of the TES and its integrated heat pump as the techno-economic potential for the HP_{direct} is very small. The total heat pump capacity also increases steadily as the

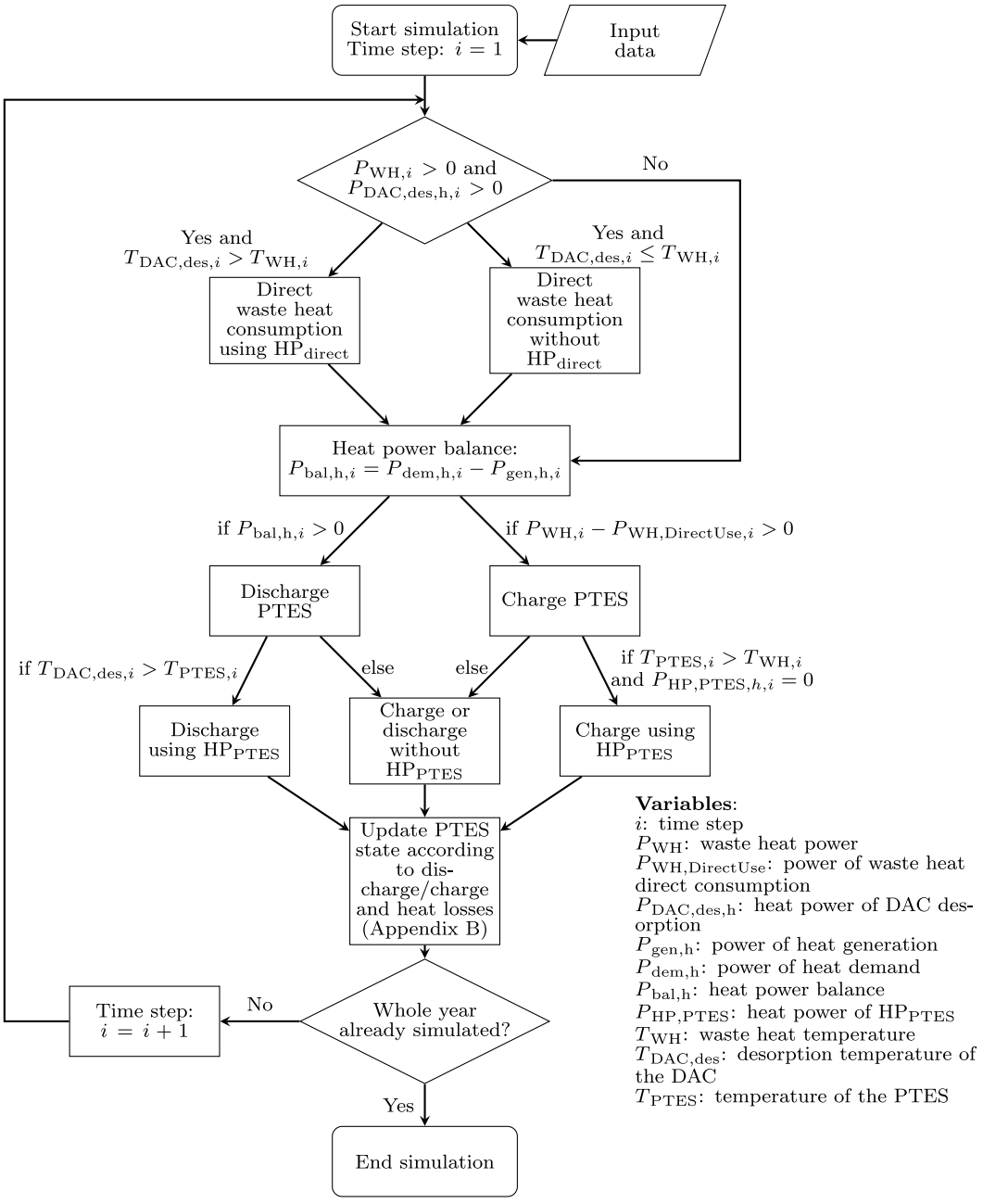


Fig. 4. Simplified flowchart of the simulation process. The simulation runs at an hourly resolution, which corresponds to 8760 time steps per year. The use of the $\mathrm{HP_{PTES}}$ is prioritized in the discharging process of the PTES. When using a heat pump, the heat transfer may be limited by the heat pump capacity. However, when a heat pump is not required, the heat transfer is assumed to be unconstrained. In practice, this means that the heat exchangers are assumed to be designed for the maximum heat transfer.

Table 3
Cost assumptions used in the study for the base case. The entire system lifetime is set to 20 a. Additionally, a 6% discount rate is used, which is close to the values typically used in techno-economic analyses of DAC [13,20,29,30]. All costs delineated in the study are exclusive of VAT. Waste heat is assumed to be cost-free, but its integration into the DAC plant requires investments.

Component	CAPEX	OPEX, fixed	OPEX, variable	Lifetime	Source
DAC plant: sorbent	40 €/kg	5% of CAPEX/a	–	2 a	[20,56,57]
DAC plant: other equipment	25% of sorbent CAPEX	5% of CAPEX/a	–	20 a	[23,56,57]
PTES	Appendix B	0.368 €/m^3/a	–	20 a	[58–60]
Heat pump	0.6 €/W_h	2850 €/MW_h/a	1.75 €/MWh_h	20 a	[61]
Electric boiler	0.15 €/W_h	500 €/MW_h/a	0.2 €/MWh_h	20 a	[61]
Electricity	–	–	Spot price (+11 €/MWh_e if import) (Appendix C)	–	–

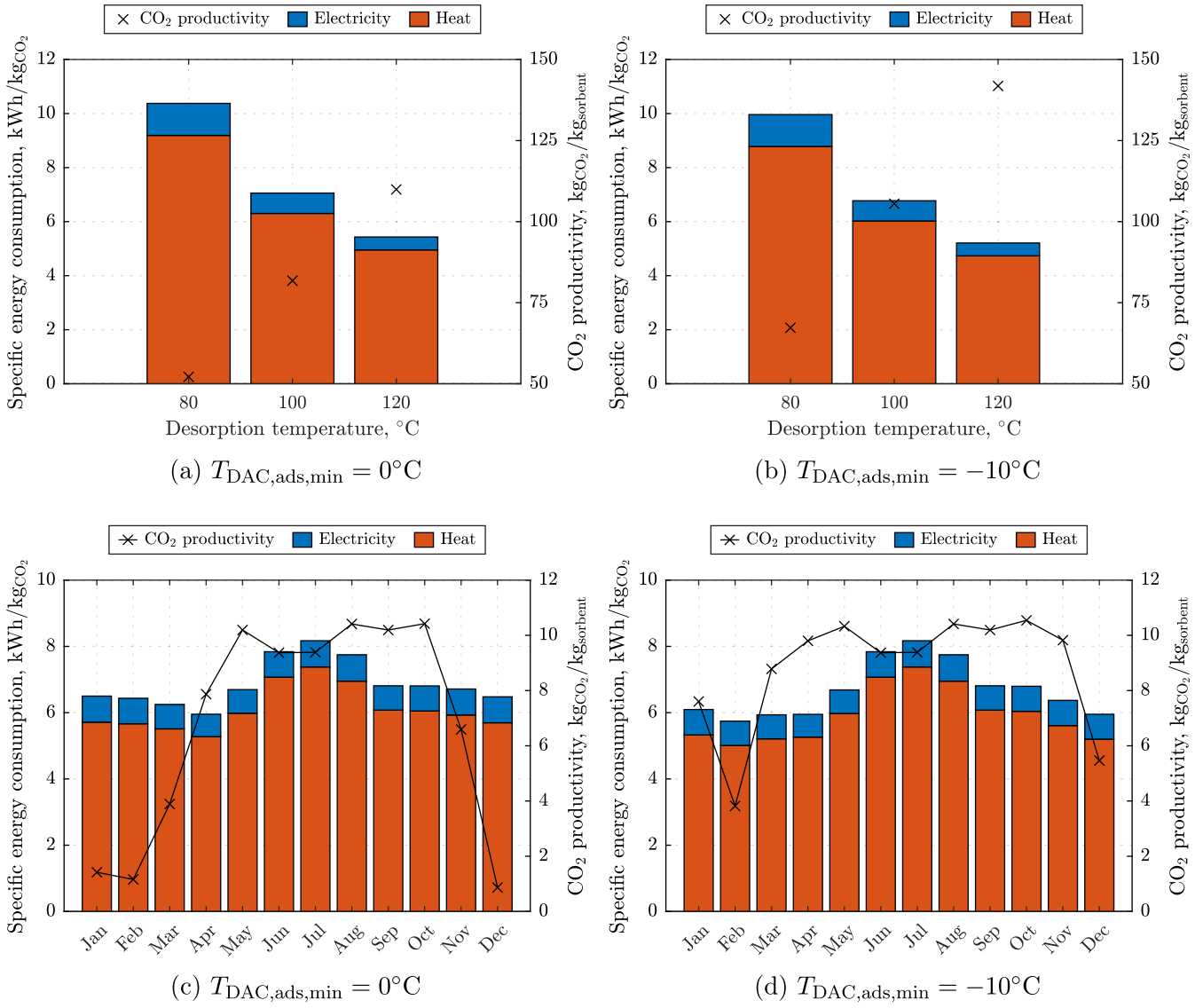


Fig. 5. Specific energy consumption and CO_2 capture of the DAC plant with two different minimum adsorption temperatures (0°C and −10°C); (a) and (b) on an annual basis as a function of desorption temperature; (c) and (d) on a monthly basis for the desorption temperature of 100°C.

desorption temperature increases, which is explained by the increase in the capacity of the DAC plant and its ability to achieve higher CO_2 productivity. Thus, even though the specific energy and power consumption decrease, their absolute values increase as the capacity and CO_2 productivity of the DAC plant increase. The slight increase in the sorbent mass in the DAC plant as a function of desorption temperature can be explained by the decreasing SEC of the DAC process and the requirement to recover at least 95% of the available waste heat from the AWE plant. When the SEC of the DAC decreases, a higher DAC system capacity (more sorbent) is required to utilize the available waste heat. The energy capacity of the PTES appears to be nearly constant across the different desorption temperatures. The nearly constant energy capacity of the PTES can be explained by the increased temperature lift of the HP_{PTES} as the desorption temperature of the DAC rises. This reduces the COP of the heat pump, increasing its electrical energy demand. Because the thermal output of a heat pump equals the sum of the thermal power extracted from the heat source and the electrical power consumed by the heat pump, the energy discharged from the PTES remains approximately the same across the different desorption temperatures annually. This, however, applies to the energy capacity of the PTES, and not to its volume, which ranges from about 180 000 to 444 000 m^3 across the cases studied. As the temperature lift increases, discharging the PTES deeply is no longer cost optimal, and the minimum temperature of the PTES therefore rises (from 19°C–26°C to 32°C–39°C), whereas its maximum temperature remains close to the temperature of the waste heat. Storing the same amount of energy over a narrower temperature range requires a larger volume, which is why the volume of the PTES increases with the desorption temperature. The most notable impact on system dimensioning arises from the minimum adsorption temperature, and the capacities of the PTES and the DAC plant decrease notably when a minimum adsorption temperature of −10°C instead of 0°C is used. The reason for this is that the operating hours of the DAC plant increase, and it can use the available waste heat with a lower capacity. For the same reason, the capacity of the PTES is reduced because waste heat generation does not need to be shifted from winter to summer to a significant extent. With the above-mentioned capacity of the DAC plant, waste heat from the 100 MW_e off-grid AWE plant, and the weather conditions in southeastern Finland, up to 27 kt/a of CO_2 can be captured, as presented in Table 4. Table 4 also shows that the annual CO_2 capture is slightly lower with a minimum adsorption temperature of −10°C than with 0°C. This is again explained by the heat pumps and their COP: the recovered waste heat is practically the same

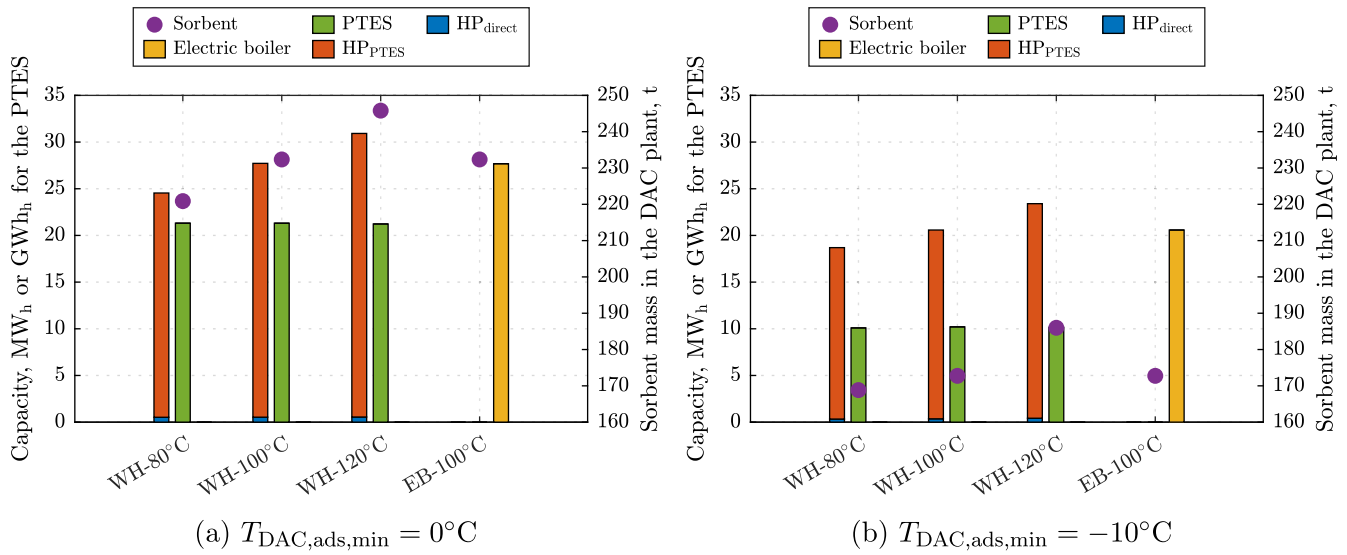


Fig. 6. Cost-optimized capacities of the waste heat recovery system with two different minimum adsorption temperatures (0°C and −10°C) at desorption temperatures of 80°C, 100°C, and 120°C. WH refers to waste-heat-based heat supply and EB to electric-boiler-based heat supply.

Table 4
Annual carbon capture and specific sorbent mass (sorbent mass per annual CO_2 capture) of the DAC plant when the heat supply is based on the waste heat from the 100 MW_e off-grid AWE plant.

Minimum adsorption temperature, °C	0			−10		
Desorption temperature, °C	80	100	120	80	100	120
CO_2 capture, kt/a	11.5	19.0	27.0	11.4	18.2	26.4
Specific sorbent mass, kg/(t_{CO_2}/a)	19.2	12.2	9.1	14.9	9.5	7.0

with both temperature limits, but the heat supplied to the DAC plant also includes the electricity consumed by the heat pumps, which differs between the two cases. As the PTES is operated at a higher temperature on average (see Fig. 10), the average temperature lift of the HP$_{PTES}$ decreases, its annual average COP increases, and less electricity is thus converted into heat for the DAC plant.

Fig. 7 illustrates the levelized cost of DAC for the DAC plant under different scenarios. The electric-boiler-based reference is simulated at the desorption temperature of 100°C, and therefore, the comparison between the heat supply scenarios is conducted at that temperature. Waste-heat-based heat supply can substantially reduce the LCODAC; by about 21%–26% with the minimum adsorption temperature of 0°C and by about 31%–36% with the minimum adsorption temperature of −10°C. A major share of the LCODAC is attributable to electricity and heat supply; therefore, halving the sorbent cost only moderately reduces the LCODAC. This reduction is about 16%–18% for the electric-boiler-based heat supply and about 21%–25% for the waste-heat-based heat supply. Under these scenarios, increasing the operating hours by enabling the minimum adsorption temperature of −10°C instead of 0°C appears to reduce the LCODAC by about 6%–9% with the electric-boiler-based heat supply and by about 18%–21% with the waste-heat-based heat supply. However, the desorption temperature has the greatest effect on the LCODAC in the waste heat scenarios; the LCODAC decreases by approximately 27%–30% when increasing the temperature from 80°C to 100°C, and by approximately 17%–20% when increasing it from 100°C to 120°C. This is interesting because, at the same time, the temperature lift of the heat pumps increases and the COP decreases. The resulting decrease in the COP increases the levelized cost of heat (LCOH) supplied, as shown in Fig. 8. Every 20°C increase in the desorption temperature increases the LCOH by approximately 13%–18%. However, the increase in the LCOH has a minor effect on the LCODAC compared with the significant improvement in DAC performance as the desorption temperature increases (see Fig. 5). It is also noteworthy that the LCOH with waste-heat-based heat supply decreases when the minimum adsorption temperature is reduced from 0°C to −10°C. This is because the capacity of the PTES is reduced (see Fig. 6), and the profitability of the heat pumps increases with increased operating hours. A similar effect is not observed in the electric-boiler-based heat supply, because the electricity purchase accounts for most of the LCOH, and its share in the LCOH cannot be reduced by increasing the operating hours of the electric boiler. In this case, the LCOH of the electric-boiler-based heat supply even increases as the average price of purchased electricity rises due to increased operation during high-price hours (see Appendix C). This also explains why the LCODAC with electric-boiler-based heat supply in Fig. 7 does not decrease significantly when the lower minimum adsorption temperature is enabled, under the hourly electricity price profile used in this study. However, integrating a small TES with an electric boiler would allow the electric boiler to operate during the least-cost hours of the day. The electric boiler is the most expensive reference for the heat supply. A brief comparison with an air-source heat pump and with waste heat at other temperatures at $T_{DAC,des}$ = 100°C is therefore presented in Appendix F (Fig. F.1). According to this comparison, an air-source heat pump also clearly reduces the LCODAC compared with the electric boiler, and the additional cost benefit of the waste heat recovery is thus smaller than that obtained against the electric boiler.

Fig. 9 compares the primary energy demand and the peak electrical power of the DAC plant between the electric-boiler-based and waste-heat-based heat supply scenarios. With the electric boiler, the primary energy demand equals the energy demand of the DAC process, whereas waste-heat-based heat supply can substantially reduce the primary energy demand of the DAC plant. By recovering waste heat from the off-grid AWE plant, the primary energy demand can be reduced by about 62%. In the case of waste heat, the primary energy demand comprises only the electricity demand of the DAC process and the electricity demand of the heat pumps. Electricity demand is primarily met by imported electricity, even though surplus electricity generation from the AWE plant is significant and could, on an annual basis, meet up to about 74% of the total electricity demand. However, its low full load hours and high variability (see [41]) indicate that it cannot be used directly without electricity storage, and thus, it has the potential to supply only 16%–19% of the total electricity demand. In addition, the peak electricity demand of the DAC plant can be reduced by about 57%, which provides a significant benefit from the perspective of the power

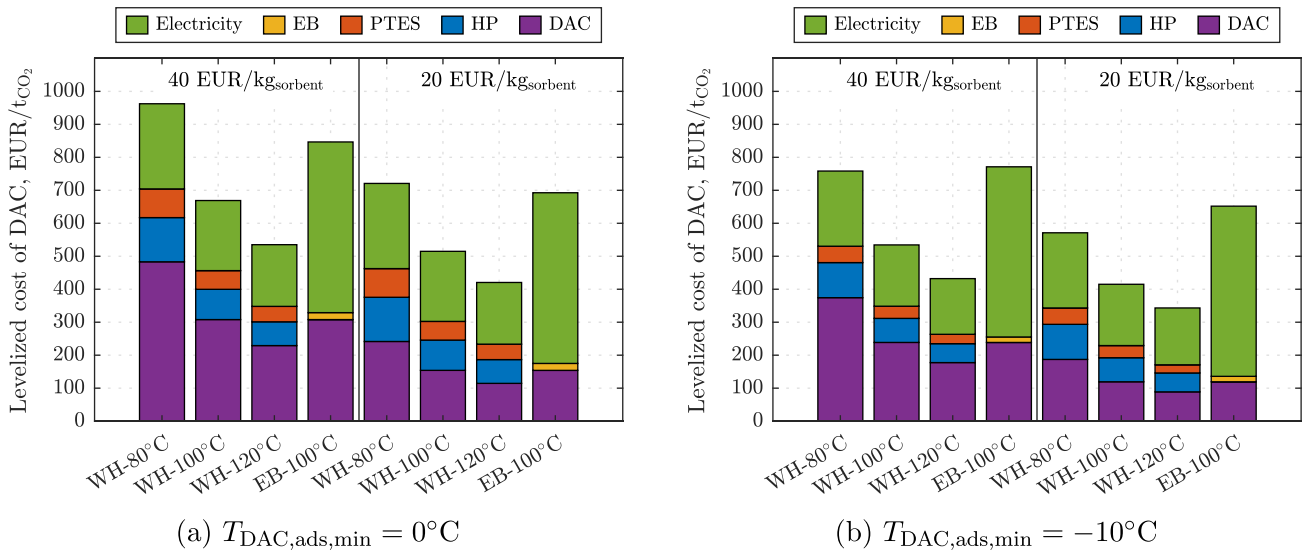


Fig. 7. Levelized cost of DAC with two different minimum adsorption temperatures (0°C and −10°C) and two different sorbent costs (40€/kg$_{sorbent}$ and 20€/kg$_{sorbent}$) at desorption temperatures of 80°C, 100°C, and 120°C. WH refers to waste-heat-based heat supply and EB to electric-boiler-based heat supply. Additionally, Appendix D provides a sensitivity analysis of the LCODAC as a function of discount rate and sorbent lifetime including a breakdown of the LCODAC by cost component.

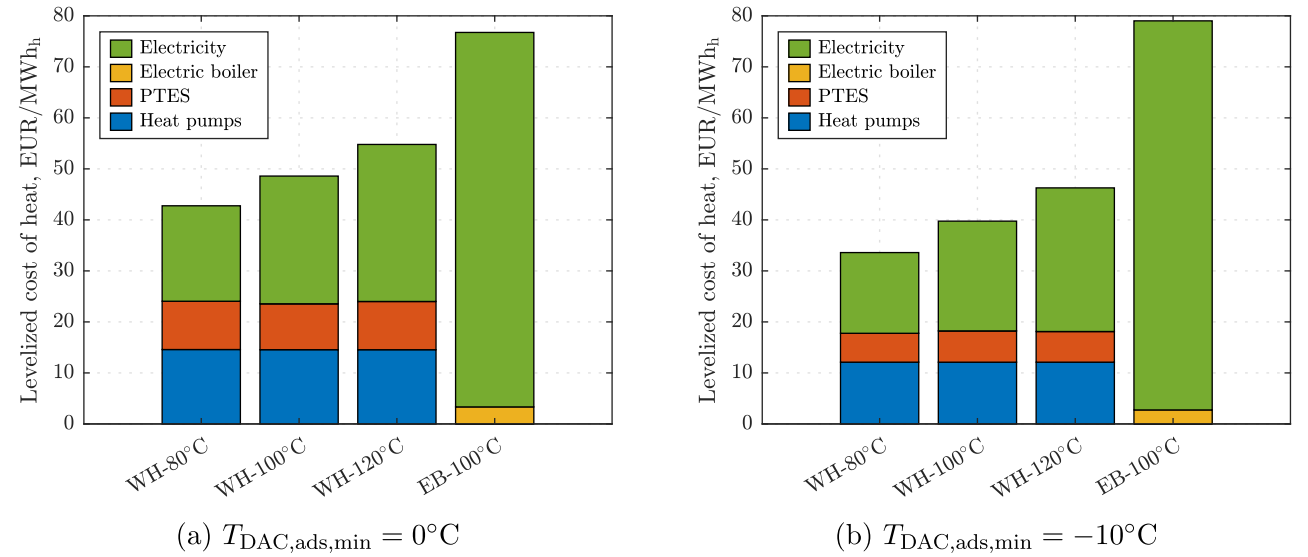


Fig. 8. Levelized cost of heat supplied to the DAC with different minimum adsorption temperatures (0°C and −10°C) at desorption temperatures of 80°C, 100°C, and 120°C. WH refers to waste-heat-based heat supply and EB to electric-boiler-based heat supply.

system. Fig. 9 is also consistent with previous observations: the DAC plant can be operated at a lower total power to utilize the available waste heat if the minimum adsorption temperature is −10°C rather than 0°C.

An example of the behavior of the waste heat recovery and heat supply for the DAC is illustrated in Fig. 10 for the desorption temperature of 100°C and for both minimum adsorption temperatures. The figure shows the hourly behavior of the DAC and its heat demand. The demand for heat power is higher in summer due to the higher ambient temperature, which increases the SEC (see Fig. 2). In addition, depending on the minimum adsorption temperature used, the DAC plant is shut down for extended periods in winter. Most of the available waste heat is used to charge the PTES directly (yellow), whereas the HP_{PTES} is employed to supply waste heat to the PTES when possible, increasing the temperature of the PTES above 70°C (March in Fig. 10). Only a very small fraction of the available waste heat is consumed directly using the HP_{direct} (blue). Consequently, most of the waste heat supplied to the DAC plant is routed through the PTES (red), enabling efficient use of the PTES and its integrated heat pump, as both components are required when the waste heat source is variable and at low temperature. It is also noteworthy that the PTES functions as a seasonal TES that is mostly discharged in summer and charged between autumn and spring. Typically, a seasonal TES stores heat from summer to winter, but a DAC operating under Nordic conditions experiences the greatest heat demand in summer, reversing the typical seasonal pattern. The waste heat that is not recovered under the 95% recovery rate is also visible in Fig. 10. It occurs in March and April, when the PTES is at its highest temperature: direct charging is no longer possible, as the storage has reached the temperature of the waste heat, and in most of these hours the HP_{PTES} is discharging the PTES to supply the DAC plant and is therefore not available for charging it. Recovering this heat would require a larger PTES, so that direct charging would remain possible for longer, or there should be heat pump capacity reserved for charging, which the configuration studied here does not provide, as

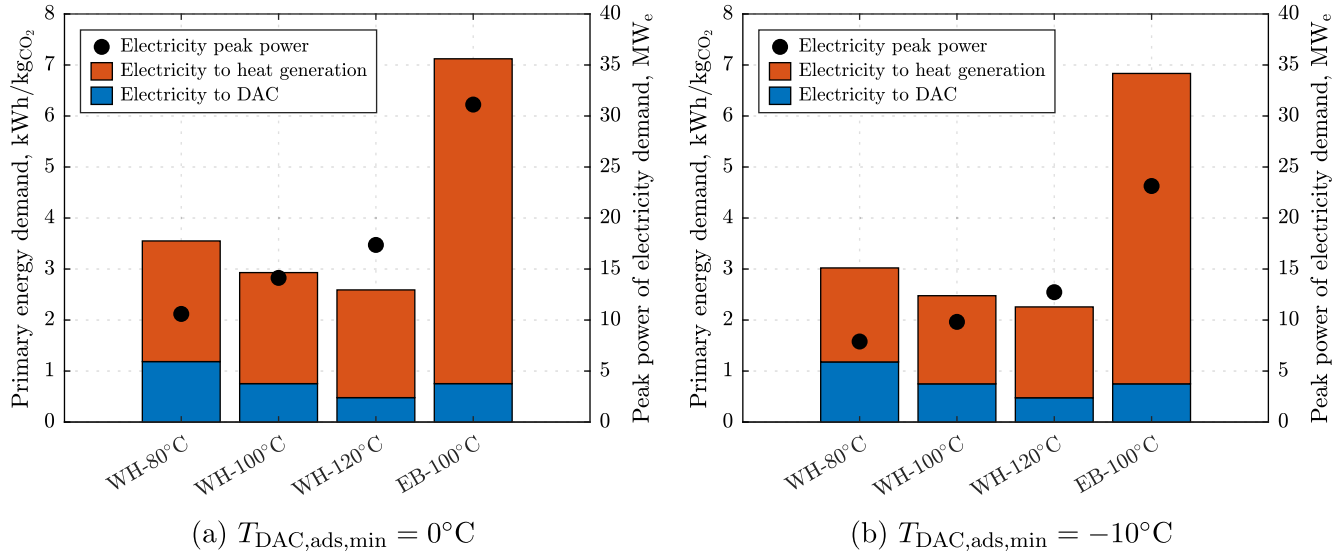


Fig. 9. Primary energy demand of the DAC plant and the peak power of electricity demand of the system with two different minimum adsorption temperatures (0°C and −10°C) at desorption temperatures of 80°C, 100°C, and 120°C. WH refers to waste-heat-based heat supply and EB to electric-boiler-based heat supply.

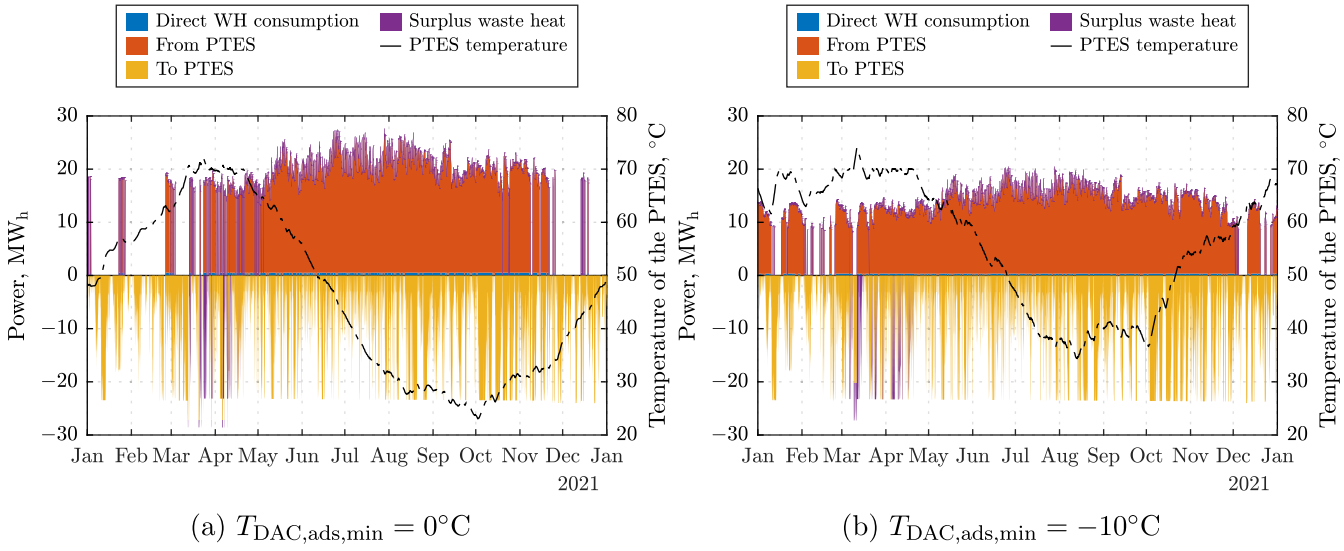


Fig. 10. Heat power supply of the DAC with two different minimum adsorption temperatures (0°C and −10°C) at a desorption temperature of 100°C at an hourly level. Additionally, Appendix E provides the hourly operation of the DAC plant, the PTES, and the HP_{PTES} separately for the case shown in (b).

a single heat pump serves the PTES in both directions. With a lower recovery rate, less CO_2 would be captured and the cost of the waste-heat-based heat supply would decrease, as a smaller recovery system operating at higher full load hours would be sufficient.

4. Discussion

4.1. Comparison with previous studies

The LCODAC achieved in this study for the electric-boiler-based heat supply (conventional scenario) is in the range of 650–845 €/t_{CO_2} while the waste-heat-based heat supply can reduce the LCODAC to 415–670 €/t_{CO_2} at the same desorption temperature of 100°C and with a sorbent lifetime of 2 a. The sorbent lifetime has a significant impact on the LCODAC. Reducing the sorbent lifetime from 2 to 1 a increases the LCODAC by approximately 30%–38% (up to 1100 €/t_{CO_2}). The absolute cost benefit of the waste heat recovery is, however, independent of the sorbent lifetime (about 178 €/t_{CO_2} at $T_{DAC,des}$ = 100°C), as the cost of the heat supply is unaffected by it. With the base-case sorbent cost of 40 €/kg, the relative reduction in the LCODAC is therefore 16% with a sorbent lifetime of 1 a, 21% with 2 a, and 23% with 3 a. The LCODAC values are in the range of LCOCDR values reported by Climeworks for its Orca plant: an estimate of 500–600 $/$t_{CO_2}$ (about 430–520 €/t_{CO_2}) in 2019 and an actual cost of 1000 €/t_{CO_2} in 2021 [16]. According to Climeworks, Orca's energy supply is based on geothermal heat [62], and the LCODAC achieved in this work for the waste heat scenario with a sorbent lifetime of 1 a is of a similar magnitude (920 €/t_{CO_2}). It should be noted that Orca experienced unexpected problems that led to reduced operating hours, thereby increasing capture costs [9]. In addition, the present study does not consider the cost of permanent carbon storage, whereas the cost of CO_2 transport and geological storage is about 5–55 €/t_{CO_2} [16,63], resulting in only a slight increase in the LCODAC if transportation and permanent storage of the captured carbon are considered. It must nevertheless be emphasized that the figures published by Climeworks cover the entire removal chain together with its profit, and they are therefore not a benchmark against which the LCODAC determined here should be judged. They are referred to only as an order-of-magnitude indication of the cost level of an operating FOAK solid DAC plant, and the comparison with the scientific literature below is considered more relevant. Therefore, it is informative to place these values in the context of published FOAK estimates. Sievert et al. [20] estimated the LCOCDR of 1282 $/$t_{CO_2}$ (about 1090 €/t_{CO_2}) for solid sorbent DACCS at the scale of the first commercial plants, falling to 374 $/$t_{CO_2}$ (about 320 €/t_{CO_2}) once a cumulative capacity of 1 Gt_{CO_2}/a is reached. With a sorbent lifetime of 1 a, the LCODAC obtained here is essentially at the FOAK level of this estimate, whereas with a sorbent lifetime of 2 a it falls below it, which supports the interpretation that the cost assumptions of this study approximate present-day rather than mature conditions. Breaking the LCODAC down by cost component shows how sensitive this balance is to the sorbent lifetime (Appendix D). With a sorbent lifetime of 1 a, the CAPEX and OPEX of the DAC plant itself, that is, the sorbent, the other equipment, and the fixed OPEX, account for 51%–61% of the LCODAC (about 560 €/t_{CO_2}), the electricity supplied to the DAC process for 5%–6% (about 55 €/t_{CO_2}), and the heat supply for 33%–44% (about 306–484 €/t_{CO_2}), the ranges spanning the two heat supply scenarios. With a sorbent lifetime of 2 a, the corresponding shares are 36%–46% (about 310 €/t_{CO_2}), 7%–8% (about 55 €/t_{CO_2}), and 46%–57% (about 306–484 €/t_{CO_2}). Terlouw et al. [13] reported a combined equipment-related CAPEX and OPEX of approximately 605 €/t_{CO_2} for the DAC plant, which is close to the value obtained here with a sorbent lifetime of 1 a. Wijesiri et al. [22] reported a similar share, with the contactors, the sorbent, and the other equipment-related costs of the DAC plant accounting for about 61% of the LCODAC, which corresponds to the upper end of the range obtained here with the same sorbent lifetime. In addition, the reduction in the SEC (or primary energy demand) of DAC when using waste heat as the heat supply instead of an electric boiler (Fig. 9) is very close to the reduction reported by Ge et al. [34].

In general, several studies assume that the heat supply for DAC is low-cost (between 20 and 50 €/MWh_h) or even cost-free in the case of waste heat [13,22,30,56]. It should be noted that the utilization of waste heat sources cannot be assumed to be free, as the cost of integration and utilization of the heat sources depends on the temperatures of the waste heat source and the heat demand, especially given that most waste heat generated in the European Union (EU) and globally is at low temperature and available at <100°C [37,38]. Furthermore, because heat generation accounts for a significant share of the LCODAC, declining investment costs of DAC technology will only moderately reduce the LCODAC, especially when the sorbent lifetime is more than one year; this limited impact will become more pronounced in the future as the DAC technology scales up and the specific investment cost continues to decrease. Therefore, it could be beneficial to design DAC systems that enable direct and cost-effective utilization of low-temperature waste heat sources. According to Appendix F, waste heat at or above the desorption temperature would reduce the LCODAC by a further 17%–19% compared with waste heat at 70°C. It should also be noted that the comparison with the electric boiler represents the upper end of the benefit of waste heat recovery, as the benefit is smaller when compared with an air-source heat pump. This comparison is, however, only indicative: the air-source heat pump is modeled optimistically, whereas the waste heat recovery system is dimensioned to recover 95% of the waste heat in order to determine the maximum CO_2 capture, which necessitates seasonal storage and thus increases the LCOH. The results also indicate that increasing the operating hours of the DAC by 31% by enabling the adsorption down to −10°C instead of 0°C can reduce the LCODAC by 6%–21%, showing that the economic benefit is not directly proportional to the required increase in operating hours. It should also be noted that allowing DAC operation down to −10°C instead of 0°C may introduce additional costs related to freeze prevention, material durability, and increased maintenance requirements. These costs are difficult to quantify, particularly given the uncertainty associated with estimating the overall costs of DAC. However, the reduction in the LCODAC reported above defines the margin that is available for them: operation down to −10°C is economically justified only if the additional costs remain below 41–75 €/t_{CO_2} with the electric boiler and 77–204 €/t_{CO_2} with waste heat. Because this margin can be modest, any increase in CAPEX or OPEX would further limit or even eliminate the economic benefit achieved through increased operating hours.

4.2. Uncertainties in the technical and economic assumptions

From the technical perspective, the SEC of the DAC model used here is considerably higher than the values reported in recent scientific studies [7,13,15,30] (5.2–10.4 kWh/kg_{CO_2} vs. even less than 3 kWh/kg_{CO_2} under optimal conditions). Climatic and weather conditions used in different studies can significantly impact the SEC, as can technological development and modeling assumptions. For example, Climeworks claims that its third-generation DAC technology doubles the CO_2 productivity per module and halves the energy consumption compared with the previous-generation technology [64]. Considering the DAC model used in this study, its energy efficiency could be increased, for example, by recirculating heat within the process to reduce thermal energy input [65] and by varying process parameters, such as cycle times, on daily and seasonal timescales based on weather conditions [30]. It should be noted that the SEC of the DAC may affect the conclusions, especially from the perspective of the costs of heat supply, in this and other studies. In this study, the contribution of heat supply to the LCODAC may be overestimated because of the high SEC. However, this does not affect the primary objective or the main findings of the study, namely the comparison between electric-boiler-based and waste-heat-based heat supply scenarios. Nevertheless, the

results demonstrate that the LCODAC is highly sensitive not only to the cost of heat supply but also to other key parameters, particularly sorbent lifetime and the discount rate.

The cost assumptions for the new technology (DAC) introduce significant uncertainty into the results, particularly regarding the absolute level of LCODAC. In this work, the CAPEX of the DAC is related to the amount of sorbent required, but in several other studies, CAPEX has been calculated based on the annual CO_2 capture capacity (the unit of the specific investment cost is €/(t · a)) [7,23,30]. Because the annual CO_2 capture capacity of DAC is strongly dependent on climatic and weather conditions, using a specific investment cost based on annual CO_2 capture capacity can yield noncomparable outcomes if the annual CO_2 capture capacity is not determined in a standardized manner (an idea comparable with standard test conditions for solar PV). Furthermore, as Appendix D presents, the discount rate used in the calculations has a significant impact on the LCODAC in the waste-heat-based heat supply scenario, which is more capital-intensive and experiences a lower OPEX compared with the electric-boiler-based heat supply. Varying the discount rate has only a moderate impact in the electric boiler scenario, as it is more OPEX-intensive and most of the costs will occur in the future (electricity purchase and sorbent replacement). Considering the OPEX of DAC, the most significant uncertainty is related to the lifetime and cost of the sorbent. In addition to the costs and lifetime of the sorbent, sorbent degradation prior to replacement can significantly affect the LCODAC [66]. For example, desorption temperatures above 100°C can cause stability problems and degradation for some amine-based adsorbents [11]. In any case, the uncertainty in DAC cost assumptions is expected to have a limited impact on the main results and conclusions of the study, which concern the techno-economic comparison of electric-boiler-based and waste-heat-based heat supply scenarios, as the costs associated with heat supply technologies are significantly more reliable.

4.3. Implications for the energy system and sector coupling

The results indicate that the 100 MW_e off-grid AWE plant producing 6.3 kt/a of baseload H_2 can provide the heat supply for a solid DAC plant capturing about 11–27 kt/a of CO_2 depending on the adsorption and desorption temperatures. Combining this CO_2 with the H_2 produced would theoretically yield about 10 kt/a of methane or 20 kt/a of methanol [67,68], and in both cases the CO_2 would be the limiting factor, leaving part of the H_2 unused. Improvements in the energy efficiency of water electrolysis would result in reduced waste heat output and can therefore further limit the capture of CO_2 in this kind of electrolyzer-DAC integration; in such cases, recovering waste heat from the synthesis process could increase CO_2 capture. However, improvements in the energy efficiency of DAC would most likely lead to the opposite situation, where H_2 becomes the limiting factor, in which case the captured CO_2 could be used in other applications or stored in a permanent carbon storage. On the other hand, overcapacity allows the DAC plant to operate based on the availability of electricity.

The availability of electricity and the required electrical grid capacity are increasingly important factors as the energy systems are electrified and more wind and solar PV power generation is integrated into the electricity system. Sector integration is a key factor for the overall efficiency of a renewable energy system, enabling both resource and cost efficiency. As shown in Fig. 9, the primary energy demand of the DAC process can be reduced by about 62% if the heat supply of the DAC plant is based on recovering waste heat from the AWE plant instead of using an individual electric boiler. Because power is the most important factor affecting the dimensioning and thereby the investment costs of the electricity system, understanding the loads connected to the electrical system and their power impact is even more important than energy efficiency. The results (Fig. 9) show that the peak power demand of the DAC process can be reduced by about 57% if waste-heat-based heat supply is used instead of an electric boiler, and also the desorption temperature of the DAC has a significant impact on the peak power demand. The lack of available connection capacity in the electricity system is a growing problem, making solutions that reduce the need for electrical power essential and potentially even vital for project implementation. If DAC plants are connected to the electricity system on a large scale, waste heat utilization may even be considered necessary. On the other hand, DAC plants can be geographically located almost anywhere and therefore have the potential to operate in an off-grid configuration, which could minimize negative impacts on the electricity system but also introduce other challenges, such as the capacity factor.

The cost-optimized PTES is large, 180 000–444 000 m^3, but of the same order as the largest units already built or planned. With the geometry assumed in Appendix B, these volumes correspond to land requirements of about 0.9–1.7 ha and to depths of about 19–26 m. The annual energy efficiency of the PTES is about 93%–96%, similar to the values obtained in the authors' previous studies [40,41]. The largest PTES units in operation, in Denmark, are of the order of 200 000 m^3 [69], while larger projects, in the range of 500 000–1 300 000 m^3, are being developed in Finland [70].

Most of the results obtained in this study can be broadly applied across different regions, although the results are representative of the Nordic context. Absolute values, such as SEC and LCODAC, are region-specific, but the relative changes presented in this study also apply elsewhere. In warmer regions, the thermal energy demand of DAC increases, which only improves the profitability of waste heat integration compared with an electric boiler. However, the practical implementation of sector-coupled energy integrations involves several challenges. Different sectors respond to their own market conditions, which can be reflected in a mismatch between waste heat generation and heat demand profiles. This mismatch can be mitigated through energy storage, although at the cost of increased system complexity and operational requirements, as the overall sector-coupled system must respond to both electricity market and end-product market signals, for example at a 15-minute resolution, while satisfying process constraints on even shorter timescales. In addition, projects are often independently owned and developed, with potentially differing investment timelines, which may limit scalability. Nevertheless, the required technologies are largely mature, and the results of this study indicate that a clear economic incentive for waste heat integration already exists, particularly compared with an electric boiler.

4.4. Limitations of the study

It should be noted that the analysis is based on system-level modeling with simplified representations of subsystems, and therefore does not capture all process-level dynamics or operational constraints. However, it can be reasonably assumed that the developed system-level model achieves sufficient technical accuracy, as it builds on an experimentally validated DAC model [11], measured data from wind, solar PV, and industrial AWE systems [42,47], and TES and heat pump models based on well-established thermodynamic principles [40,41]. Validation is ensured by verifying power and energy balances at both subsystem and system levels, as already performed in two previous publications at 5-minute and 15-minute time resolution [40,41], since experimental validation at this scale is not feasible. In addition, uncertainties related to DAC cost assumptions, sorbent performance, and long-term degradation remain significant. Ultimately, economic assumptions, which are inherently project-specific input parameters, may have a greater impact on the results than possible inaccuracies in the simulation models.

Furthermore, the analysis is based on a single weather and power generation year (2021), which is also the year for which the off-grid AWE plant was cost-optimized, so that the waste heat profile, the ambient conditions of the DAC plant, and the electricity prices are mutually consistent. A multi-year analysis would give a more complete picture

of the interannual variability of the CO_2 capture and of the required PTES capacity, and the use of a single year is therefore recognized as a limitation. Both heat supply scenarios are, however, exposed to exactly the same conditions, and the relative comparison between them, which is the primary objective of this study, is not expected to be sensitive to the choice of the year.

The cost boundary on the waste heat extraction side should also be made explicit. The system considered here begins at the cooling circuit of the AWE plant, and the costs of the heat pumps, the PTES, the electric boiler, and the electricity purchased by these components are all included. The investment costs of the heat pumps, the PTES, and the electric boiler cover installation costs in addition to the equipment cost itself, and therefore also the components required for system integration, such as heat exchangers and piping [59,61]. The AWE and the DAC plants are assumed to be co-located, so that no long heat transmission pipelines are required. On the AWE side, the waste heat recovery replaces most of the duty of the original heat rejection system of the electrolyzer plant, as only about 5% of the released heat has to be rejected by the original cooling system with the recovery rate of 95% applied here. This is nevertheless not treated as an avoided investment. An independent cooling system would most probably have to be retained so that the electrolyzer plant can be operated when the DAC plant is unavailable, for example during maintenance or a fault, and it would then still have to be dimensioned for the full heat rejection duty. What the waste heat recovery avoids is thus mainly the cost of the auxiliary electricity consumed by the fans and pumps of the original cooling system, rather than its investment cost. This saving accrues to the operator of the electrolyzer plant rather than to the DAC plant, and it is what makes a zero price for the waste heat at the boundary of the AWE plant a reasonable assumption: the heat itself is provided free of charge, whereas the cost of recovering and upgrading it is fully accounted for on the DAC side.

4.5. Future research

Future research could focus on more detailed process-level modeling, experimental validation, and integration of DAC into broader sector-coupled energy systems, with the aim of understanding how sector coupling can be realized in practice, as this feasibility study has demonstrated significant techno-economic benefits of waste heat recovery at the system level. In addition, building-integrated DAC has the potential to reduce the cost of carbon capture due to increased CO_2 concentration levels [15]. Therefore, it would be important to understand how waste-heat-based heat supply is implemented cost-optimally in cities.

5. Conclusions

This study examined the techno-economic potential of recovering waste heat from water electrolysis for use in a direct air capture (DAC) plant based on a temperature-vacuum swing adsorption (TVSA) approach. Waste heat at 70°C from an off-grid alkaline water electrolyzer (AWE) plant, cost-optimized to supply baseload H_2, for the desorption process of the DAC plant operating at 80°C–120°C, was recovered using heat pumps and a pit thermal energy storage (PTES). The methodology developed in previous studies was employed to optimize the capacities of both the waste heat recovery system and the DAC plant at an hourly resolution to minimize the levelized cost of DAC (LCODAC). One of the main objectives of the work was to identify how varying the desorption temperature affects the profitability of the waste heat integration. In addition, the impact of varying DAC operating hours, achieved by changing the minimum adsorption temperature, on the profitability of DAC under Nordic conditions was investigated. A comparison between the waste-heat-based heat supply and an electric-boiler-based one was also performed to determine the techno-economic benefit of the waste heat recovery.

Generally, the feasible adsorption temperature of DAC is in the range of 0°C–30°C, and therefore the operating hours of a DAC plant under Nordic conditions are limited, because the ambient temperature in winter is usually below 0°C. This results in most of the CO_2 being captured in summer, causing the PTES to operate as a seasonal storage that shifts waste heat generated in winter to be used in summer. It was found that the $100\,MW_e$ off-grid AWE plant producing $6.3\,kt/a$ of H_2 generates waste heat that can be used to supply thermal energy for the DAC plant capturing $11–27\,kt/a$ of CO_2.

The results show that the LCODAC can be reduced by 21%–36% when the heat supply of the DAC plant is based on the AWE plant's waste heat instead of an electric boiler at the same desorption temperature of 100°C and with a sorbent lifetime of 2 a. Compared with an air-source heat pump, the cost benefit is smaller and depends on how well the availability of the waste heat matches the heat demand of the DAC plant. Heat supply was found to be the largest cost component in the LCODAC in the base case with the sorbent lifetime of 2 a. However, when the sorbent lifetime is reduced to 1 a, the capital expenditure (CAPEX) and the operational expenditure (OPEX) related to the DAC equipment become the largest cost component. Although the coefficient of performance (COP) of the heat pumps decreases as the desorption temperature of the DAC increases, higher desorption temperatures are highly beneficial from a techno-economic perspective, as the resulting increase in CO_2 productivity of the DAC is more significant than the economic loss caused by the decrease in the COP. Increasing the desorption temperature from 80°C to 100°C can reduce the LCODAC by 27%–30%, while an increase from 100°C to 120°C reduces the LCODAC by an additional 17%–20%. Operating the DAC plant at ambient temperatures down to −10°C instead of 0°C may not be economically warranted if subzero operation poses any risk of equipment freezing, as the LCODAC can be reduced by only 6%–21%, corresponding to a margin of 41–204 €/t_{CO_2} for the possible additional costs of subzero operation.

From the perspective of the electricity system, recovering waste heat for use in DAC plants is highly beneficial. It was found that the primary energy demand of the DAC plant can be reduced by approximately 62%, and the peak electrical power demand can be reduced by approximately 57%, when the heat supply is based on the AWE plant's waste heat instead of an electric boiler. Policy instruments, electricity pricing, and grid connection regulations should incentivize improvements in energy efficiency and the minimization of peak power demand in new energy-intensive applications, so that electricity and grid connection capacity can be used efficiently across different applications within electricity networks. The appropriate signal should already be in place as the waste-heat-based heat supply significantly improves the cost efficiency of solid DAC. However, such integration may not be realized in practice if industrial actors that generate and utilize waste heat are not strategically co-located. Resource- and cost-efficient sector coupling could be enabled by incentivizing the formation of industrial energy communities in locations where significant industrial by-products, such as waste heat, and renewable electricity generation potential are available. Primary energy demand and the cost of heat supply for the DAC could be further reduced if the temperatures of the waste heat source and the desorption process match. With waste heat at or above the desorption temperature of 100°C, the LCODAC would be 17%–19% lower than with waste heat at 70°C. Therefore, it could be beneficial to design DAC systems that enable direct and cost-effective utilization of low-temperature waste heat sources without the need for temperature elevation using heat pumps, in which case the primary energy demand of DAC would consist only of fans, vacuum pumps, and other balance-of-plant components. This work provides one of the first scientifically grounded insights into the integration of electrolysis-based waste heat with DAC, and the findings can support decision-making in the planning of DAC projects and associated energy infrastructure. It should also be noted that although the waste heat considered in this study is electrolysis-based, the results are applicable to other waste heat sources with similar temperature levels and generation profiles.

CRediT authorship contribution statement

Altti Meriläinen: Writing – original draft, Visualization, Validation, Software, Methodology, Investigation, Formal analysis, Data curation, Conceptualization. **Antti Kosonen:** Writing – review & editing, Supervision, Project administration, Methodology, Funding acquisition, Conceptualization. **Peter Holtappels:** Writing – review & editing, Resources, Methodology, Conceptualization. **Roland Dittmeyer:** Writing – review & editing, Resources, Methodology, Conceptualization. **Pertti Kauranen:** Writing – review & editing, Methodology, Funding acquisition, Conceptualization. **Jero Ahola:** Writing – review & editing, Supervision, Funding acquisition, Conceptualization.

Declaration of Generative AI and AI-assisted technologies in the writing process

During the preparation of this work, the authors used Anthropic's Claude Opus 5 and M365 Copilot in order to improve readability and language of the manuscript. After using these tools/services, the authors reviewed and edited the content as needed and take full responsibility for the content of the publication.

Declaration of competing interest

The authors declare that they have no known competing financial interests or personal relationships that could have appeared to influence the work reported in this paper.

Acknowledgments

Business Finland and the Strategic Research Council established within the Research Council of Finland are acknowledged for the main financial support of the B2RECoM (Business Finland grant number: 10784/31/2022) and PHOENIX (SRC grant number: 358391) projects. Furthermore, the Finnish Foundation for Technology Promotion and the Walter Ahlström Foundation are acknowledged for their financial support for the corresponding author.

Appendix A. Modeling of the heat pumps

Modeling of the heat pumps is based on the authors' previous study [41], in which the coefficient of performance (COP) and the specific heat rate as a function of temperature lift for the specific heat pumps were modeled. The same study also highlighted that detailed modeling of subsystems does not necessarily cause a significant change in the final result in a large system, but the input data (e.g., cost assumptions) used can have a much greater impact on the final result. Therefore, in the present study, heat pump performance is considered primarily in terms of COP, which varies as a function of source and sink temperatures. The dynamic specific heat rate, which was considered in [41] and depends on source and sink temperatures, is neglected and instead assumed to be constant, as it mainly affects heat pump performance under off-design conditions relative to the design point. Heat pumps are assumed to be designed for the maximum required temperature lift, and thus, at lower temperature differences (off-design conditions), their specific heat rate increases, improving performance. Heat pump cycles are modeled with the following main assumptions; a more detailed description of the modeling process can be found in [41]:

1. The refrigerant is butane, which is suitable for the temperature range considered and has been studied in large-scale heat pump systems, for example, in [24,71,72]. The thermodynamic properties of the refrigerant are obtained by using a thermodynamic property database CoolProp [73].

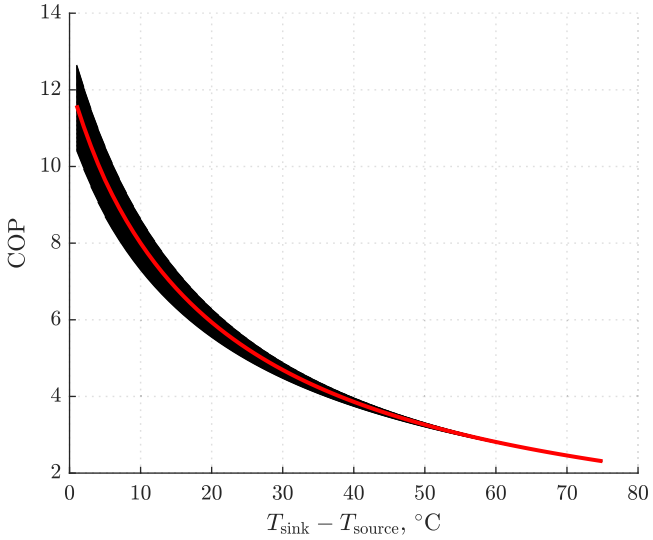


Fig. A.1. Coefficient of performance of the heat pumps [41]. The black lines indicate all the COPs as a function of temperature difference for all the different source temperatures, and the red line represents the average of the different COPs for a given temperature difference.

2. A constant mass flow of the refrigerant is assumed when the thermal power in off-design conditions is assessed. Displacement compressors are commonly used with heat pumps [74], and for a fixed-speed displacement compressor, the mass flow does not change significantly when the pressure ratio changes [75].
3. A constant compressor isentropic efficiency of 70% is used for all the operating points. Typical displacement compressors work with design point efficiencies of about 70% [74], and the efficiency changes only slightly in off-design conditions [76].
4. The evaporating temperature is 10°C lower than the heat source temperature, and the condensing temperature is 10°C higher than the heat sink temperature. It is noteworthy that the assumed temperature differences between the refrigerant and the heat sink as well as the heat source are relatively small, and higher temperature differences would slightly reduce the COP.
5. Heat and pressure losses are neglected in the model for simplification.
6. The thermal power output of a heat pump is the sum of the heat extracted from the heat source and the electricity consumed by the heat pump. The thermal power of the heat pump is limited by its capacity and the availability of the heat source.

The COP of the heat pumps is shown in Fig. A.1. As can be observed, there is slight variation in COPs for a given temperature difference, depending on the heat source temperature. The heat source temperature for the HP_{PTES} is variable, as the temperature of the pit thermal energy storage (PTES), acting as the heat source, varies as a function of its state of charge. In contrast, for the HP_{direct}, both the source and sink temperatures are constant. The effect of the heat source temperature on COP variation is minor and is mainly observed at very small temperature differences. Therefore, a single COP value is used for each temperature difference, determined as the average of all COP values for a given temperature lift, as shown by the red line in Fig. A.1. Overall, the modeled COP behaves in a manner similar to that illustrated in [24], where an experiment was conducted for a high-temperature heat pump operating in similar temperature ranges and using butane as the refrigerant.

Appendix B. Modeling and specific investment cost of the PTES

A PTES is a large-scale sensible heat storage in which water contained in an excavated pit serves as the storage medium. The pit is sealed with a polymer liner, insulated at the bottom and on the sides mainly by the surrounding soil, and covered with an insulated floating lid that limits heat losses to the ambient air [58,69]. The maximum storage temperature is limited to approximately 90°C–95°C by the durability of the liner and the insulation materials, whereas the minimum temperature is typically 10°C–20°C [58,69]. Therefore, a heat pump (or other means of temperature elevation) is required whenever the temperature of the heat demand exceeds the temperature of the storage, which is mostly the case in this study, as the desorption process of the direct air capture (DAC) requires heat at 80°C–120°C. Among the large-scale water-based storage technologies, that is, tank, pit, borehole, and aquifer thermal energy storage, the PTES has proven particularly successful, especially in Denmark, owing to its low specific investment cost, straightforward construction, and simple and inexpensive scaling to seasonal storage capacities [58,69]. The same PTES model has been applied and analyzed in more detail in the authors' previous studies on the recovery of water electrolysis waste heat into a district heating network [40,41].

The most typical PTES geometry is a truncated pyramid stump, but the pit can also be a truncated cone or a complicated pyramid setup [69]. The geometry affects not only the construction costs but also the heat losses of a PTES. According to Bai et al. [77], the difference between the heat losses of different geometries of a PTES can be up to 15%–25%. In this study, the modeling of the PTES is simplified. The PTES is assumed to be a square rectangular cuboid with the top and bottom faces being square. The height of the square rectangular cuboid is assumed to be one-fifth of the length of the side of the top square. A typical height of a large-scale PTES (60 000–200 000 m^3) is about 15–20 m [69]. Therefore, for example, a 200 000 m^3 PTES with the assumptions made in this study would be achieved with a square rectangular cuboid with the dimensions of 100 m, 100 m, and 20 m for length, width, and height, respectively. Optimization of the pit height and wall slopes for different PTES dimensioning cases has not been considered relevant for this work, but the heat losses can be assumed to be calculated sufficiently well with the assumptions made in the study.

The modeling of the PTES is based on basic thermodynamics with an assumption that the water in the pit is fully mixed (i.e., no temperature stratification) to simplify the heat loss calculation. Schütz et al. [78] compared the use of fully mixed and stratified thermal energy storage (TES) models equipped with a heat pump in the heating system optimization of a residential building and found that the fully mixed model underestimates the operating costs by 4%, while substantially reducing computational time. Therefore, the use of the simplified TES model is warranted, as it significantly reduces the computational burden without having a major impact on the final results. In addition, simultaneous discharging and charging of the PTES is allowed to enable more efficient utilization of the PTES and its integrated heat pump. Simultaneous charging and discharging of a TES is ultimately a design choice and can be implemented by using separate charging and discharging circuits (i.e., two separate heat exchangers).

The heat loss power of each face of the PTES is calculated as follows:

$$P_{\mathrm{loss},i} = U \cdot A \cdot \Delta T_i, \tag{B.1}$$

where U is the U-value of the material of the face, A is the area of the face, and ΔT is the temperature difference between the water in the PTES and ground/outdoor air. The U-values have been estimated based on the literature and are 0.4 $W/(m^2 \cdot K)$, 0.1 $W/(m^2 \cdot K)$, and 0.2 $W/(m^2 \cdot K)$ for the top, bottom, and sides, respectively [79,80]. A higher U-value is used for the top than is presented in the literature (0.4 $W/(m^2 \cdot K)$ instead of 0.186 $W/(m^2 \cdot K)$) to compensate for the smaller surface area and the losses of the top caused by the square rectangular cuboid assumption. In real-life PTES applications, the side walls are typically not vertical, leading to an increase in the area of the top cover if the height and volume of the pit remain constant. Measured hourly data from the local weather station are used to determine the outdoor air and ground temperature. For simplification, the annual average is used as the temperature of the ground, which can be determined by adding 2°C to the annual average of the outdoor air temperature [81]. According to [82], the annual average ground temperature is approximately the same at ground depths of 0–7 m, and the temperature variation between seasons is already minimal at a depth of >7 m.

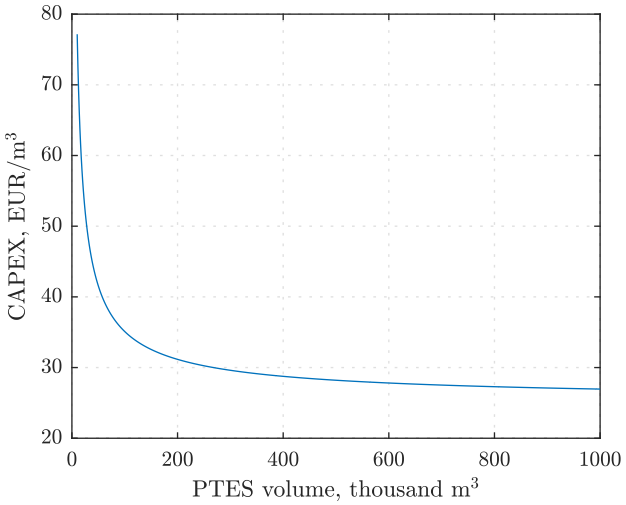


Fig. B.1. Specific investment cost of the pit thermal energy storage [40]. Approximately 70% of the CAPEX is associated with installation costs, while the equipment itself accounts for the remaining 30%.

The amount of heat transferred during the charging or discharging (or heat loss) process of the PTES is calculated according to the following equation:

$$Q_i = P_{\mathrm{h},i} \cdot \Delta t \cdot 3600, \tag{B.2}$$

where P_{h} is the heat power and Δt is the change of time in hours (1 h in this study). According to Q, the temperature change in the PTES while charging and discharging is calculated based on the energy change as follows:

$$\Delta T_{\mathrm{PTES},i} = \frac{Q_i}{\rho_{\mathrm{water}} \cdot V_{\mathrm{PTES}} \cdot c_{\mathrm{water}}}, \tag{B.3}$$

where ρ_{water} is the density of water (1000 kg/m^3), V_{PTES} is the volume of the PTES, and c_{water} is the specific heat capacity of water (4186 $J/(kg \cdot K)$). In the charging process, the PTES can be charged up to the maximum temperature, which is assumed to be 95°C. In the discharging process, thermal energy from the PTES can be discharged directly to the demand if the temperature of the PTES is higher than the temperature required in the desorption process of a DAC. If the temperature of the PTES is lower than the temperature required in the DAC, a heat pump is used to boost the temperature so that it is suitable for the desorption.

The specific investment cost for the PTES is described in Fig. B.1.

Appendix C. Electricity spot price

See Fig. C.1.

Appendix D. Sensitivity analyses

See Figs. D.1 and D.2.

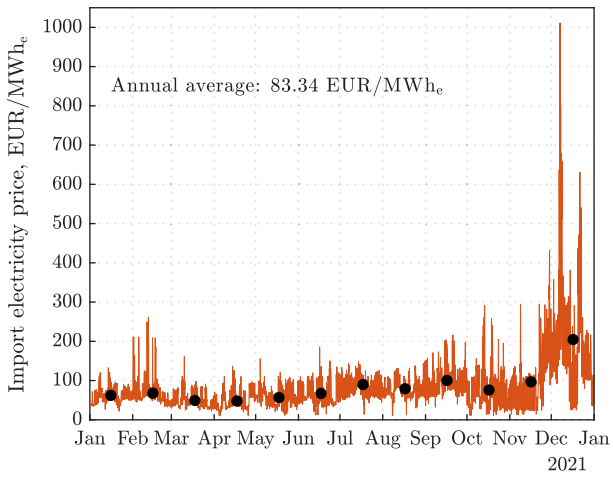


Fig. C.1. Import electricity price based on the Nord Pool day-ahead Finnish area price for the year 2021 [83], with an additional 11 €/MWh$_e$ to account for transmission costs and the electricity tax, which is a typical value for enterprise and corporate end users in Finland with the annual electricity consumption ranging from 20 to 150 GWh [84]. Monthly average prices are indicated by black markers. The price does not include the VAT or any costs related to carbon emissions. Specific CO_2 emissions from electricity generation in Finland have decreased from 75 to 26 g_{CO_2}/kWh_e between 2021 and 2025 [85].

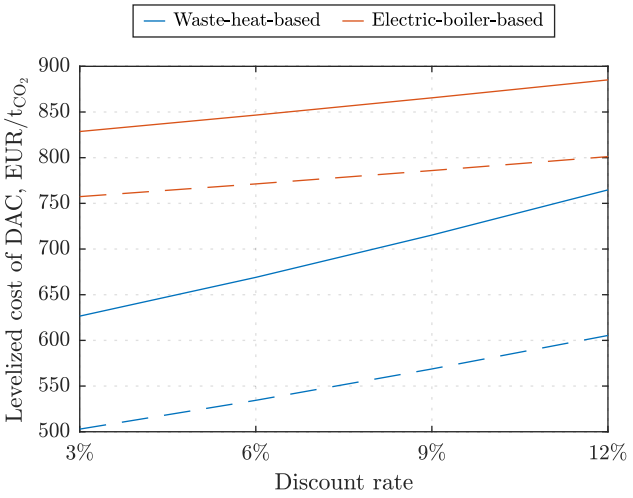


Fig. D.1. Effect of discount rate on the levelized cost of DAC for both heat supply scenarios in the base case with $T_{DAC,des}$ = 100°C. The solid line represents the LCODAC at $T_{DAC,ads,min}$ = 0°C, and the dashed line at $T_{DAC,ads,min}$ = −10°C. The optimization was performed with a 6% discount rate, and the component dimensioning and values of other parameters remain the same as in the optimized case, while the discount rate is changed.

Appendix E. Hourly operation of the subsystems

See Fig. E.1.

Appendix F. Comparison with alternative heat sources

The waste-heat-based heat supply is compared with two alternative heat sources at the desorption temperature of 100°C with the base-case cost assumptions (Table 3). First, the temperature of the waste heat is varied from 0°C to 120°C in steps of 10°C, and the system is re-optimized for each temperature with the same generation profile, system configuration, and constraints as in the main analysis. Second, an air-source heat pump without waste heat recovery or TES supplies

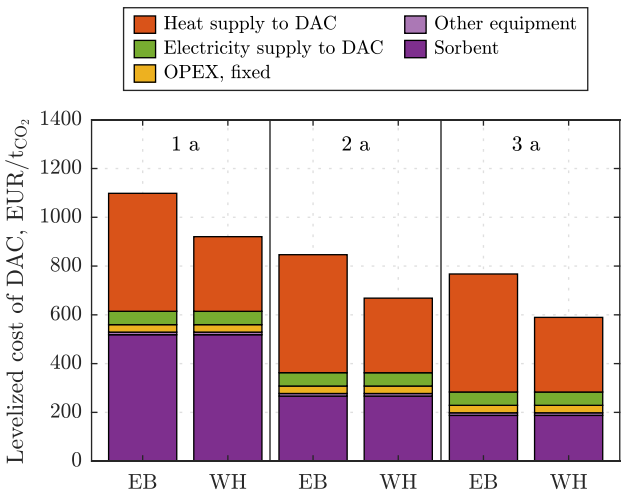
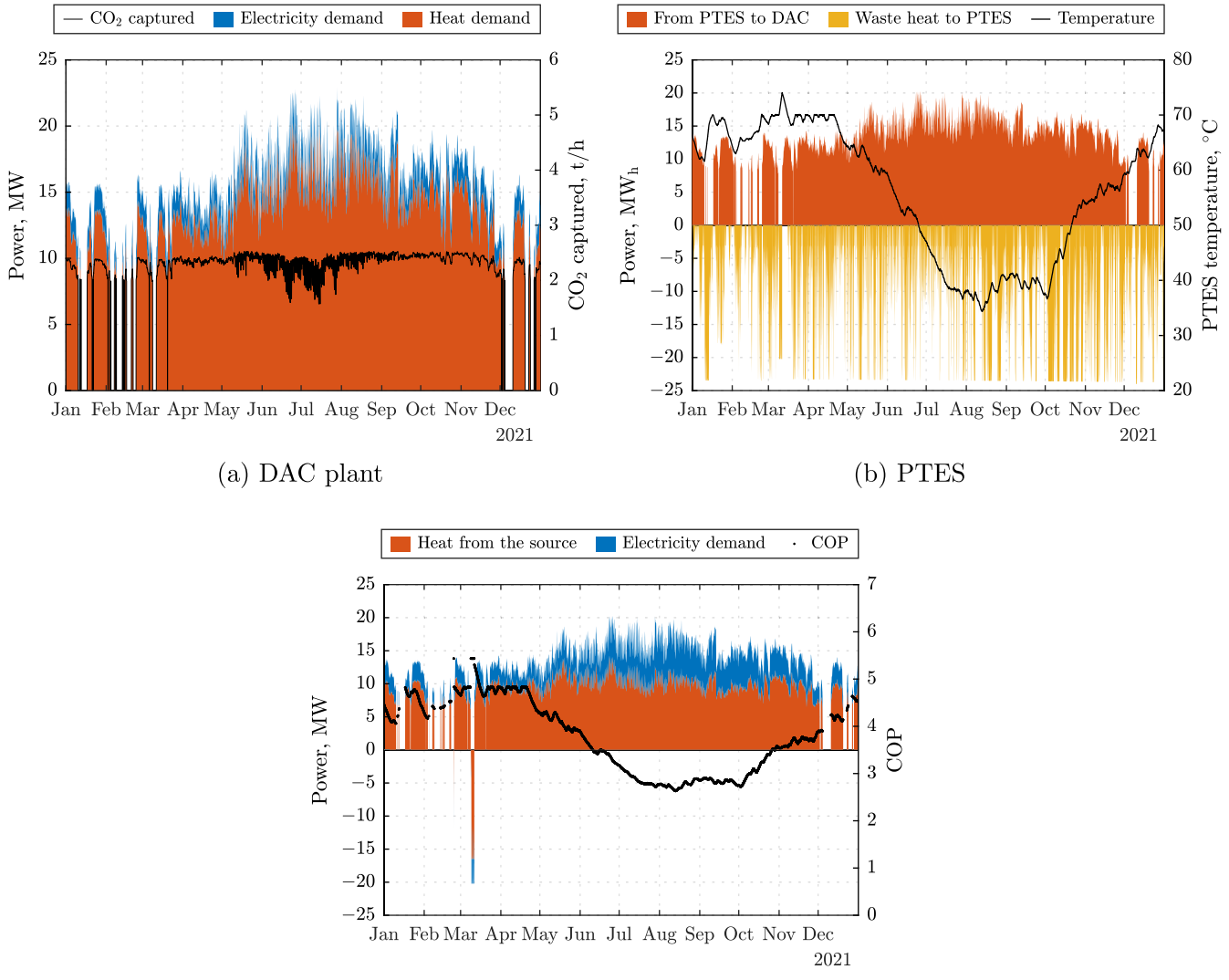


Fig. D.2. Effect of sorbent lifetime on the levelized cost of DAC for both heat supply scenarios in the base case with $T_{DAC,des}$ = 100°C and $T_{DAC,ads,min}$ = 0°C. The LCODAC and its distribution represent optimized values for sorbent lifetimes ranging from 1 to 3 years. WH refers to waste-heat-based heat supply and EB to electric-boiler-based heat supply.

the desorption heat of the same DAC plant as in the waste heat scenario at 70°C, using the hourly ambient temperature as the temperature of the heat source.

Two cases of the air-source heat pump are analyzed. The idealized case uses the COP curve (Appendix A) and the specific investment cost of the main analysis. In the more realistic case, the investment cost is increased by 10% and the COP is reduced by 10%. Large-scale air-source heat pumps are about 1%–7% more expensive than heat pumps utilizing excess heat [86,87] because of the air coolers (the heat exchangers and fans that extract heat from the ambient air), which account for about 10% of the total investment [87], and the oversizing of the evaporators for defrosting [86]. Frosting and defrosting, which are not included in the COP curve, have been reported to reduce the seasonal performance of air-source heat pumps by 2%–13% [88,89] and the COP by 11%–21% during frosting periods in a cold and humid climate [90]. As the temperature lift of the air-source heat pump (70°C–110°C) also extends beyond the range of the COP data (Fig. A.1), its results are likely to be optimistic.

The results are shown in Fig. F.1. The LCODAC and the levelized cost of heat (LCOH) decrease as the waste heat temperature increases, and with waste heat at or above the desorption temperature, the LCODAC is 17%–19% lower than with waste heat at 70°C. The air-source heat pump reaches an annual average COP of 1.7–1.9 and reduces the LCODAC by 16%–21% compared with the electric boiler. Compared with the air-source heat pump, waste heat at 70°C reduces the LCODAC by a further 2%–6% with the minimum adsorption temperature of 0°C and by 12%–16% with −10°C, and it requires 33%–52% less electricity for the heat supply. This benefit is affected by the recovery rate of 95%, which is applied to determine the maximum CO_2 capture: the waste heat generated in winter has to be stored until summer, and the PTES accounts for 15%–19% of the LCOH at 70°C. The benefit is accordingly larger with the minimum adsorption temperature of −10°C, which requires less storage. Waste heat is more cost-effective than the air-source heat pump at waste heat temperatures above approximately 45°C–65°C with the minimum adsorption temperature of 0°C and above 25°C–35°C with −10°C, depending on the air-source heat pump case. At 70°C, the LCODAC and LCOH of the re-optimized system deviate by less than 0.2% from those in Section 3, whereas the capacities differ by up to about 13% and the annual CO_2 capture by up to about 3%, owing to the stochastic optimization algorithm (Section 2.2).



(a) DAC plant

(b) PTES

(c) HP_{PTES}

Fig. E.1. Hourly operation of (a) the DAC plant, (b) the PTES, and (c) the heat pump for the PTES (HP_{PTES}) with waste-heat-based heat supply at $T_{DAC,des}$ = 100°C and $T_{DAC,ads,min}$ = −10°C. The areas in (a) and (c) are stacked, and thus, their upper boundary is the total energy demand of the DAC plant and the heat supplied by the heat pump, respectively. In (b) and (c), positive values denote discharging and negative values charging of the PTES.

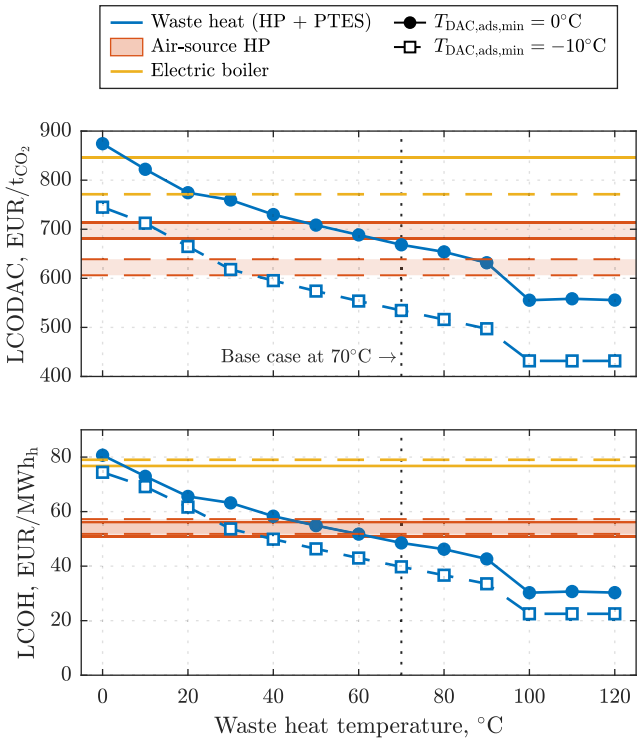


Fig. F.1. Levelized cost of DAC (LCODAC, top) and levelized cost of heat (LCOH, bottom) as a function of waste heat temperature at $T_{DAC,des}$ = 100°C with the minimum adsorption temperatures of 0°C (solid lines, filled markers) and −10°C (dashed lines, open markers). The band of the air-source heat pump spans the idealized case (lower edge) and the more realistic case (upper edge). The vertical dotted line indicates the base case with waste heat at 70°C.

Data availability

The data that has been used is confidential.

References

[1] IPCC. In: Shukla PR, Skea J, editors. Climate change 2022: Mitigation of climate change. Contribution of Working Group III to the Sixth Assessment Report of the Intergovernmental Panel on Climate Change. Tech. rep., Cambridge University Press, Cambridge, UK and New York, NY, USA: Intergovernmental Panel on Climate Change; 2022, http://dx.doi.org/10.1017/9781009157926, URL https://www.ipcc.ch/report/ar6/wg3/.

[2] Bogdanov D, Ram M, Satymov R, Lopez G, Mensah TN, Sadovskaia K, et al. Costs and benefits of highly ambitious energy transition pathways for Europe. Energy 2025;336:138477. http://dx.doi.org/10.1016/j.energy.2025.138477, URL https://linkinghub.elsevier.com/retrieve/pii/S0360544225041192.

[3] Breyer C, Lopez G, Bogdanov D, Laaksonen P. The role of electricity-based hydrogen in the emerging power-to-X economy. Int J Hydrog Energy 2024;49:351–9. http://dx.doi.org/10.1016/j.ijhydene.2023.08.170, URL https://linkinghub.elsevier.com/retrieve/pii/S0360319923041721.

[4] Seyyedattar M, Zendehboudi S. Carbon capture and storage: A comprehensive review on current trends, techniques, and future prospects in North America. Fuel 2026;407:137276. http://dx.doi.org/10.1016/j.fuel.2025.137276, URL https://linkinghub.elsevier.com/retrieve/pii/S0016236125030017.

[5] Bui M, Adjiman CS, Bardow A, Anthony EJ, Boston A, Brown S, et al. Carbon capture and storage (CCS): the way forward. Energy Environ Sci 2018;11(5):1062–176. http://dx.doi.org/10.1039/C7EE02342A, URL https://pubs.rsc.org/en/content/articlelanding/2018/ee/c7ee02342a.

[6] Breyer C, Keiner D, Abbott BW, Bamber JL, Creutzig F, Gerhards C, et al. Proposing a 1.0°C climate target for a safer future. PLoS Clim 2023;2(6):e0000234. http://dx.doi.org/10.1371/journal.pclm.0000234, URL https://dx.plos.org/10.1371/journal.pclm.0000234.

[7] Koch R, Dittmeyer R. Comparative analysis of industrialization potentials of direct air capture technologies. Front Clim 2025;7:1558396. http://dx.doi.org/10.3389/fclim.2025.1558396, URL https://www.frontiersin.org/journals/climate/articles/10.3389/fclim.2025.1558396/full.

[8] McQueen N, Gomes KV, McCormick C, Blumanthal K, Pisciotta M, Wilcox J. A review of direct air capture (DAC): scaling up commercial technologies and innovating for the future. Prog Energy 2021;3(3):032001. http://dx.doi.org/10.1088/2516-1083/abf1ce.

[9] Trompoukis C, Koponen K, Elfving J, Bajamundi C, Deliukov A, Kila A, et al. The role of direct air capture technologies in the EU's decarbonisation effort. Tech. rep., Luxembourg: Publication for the Committee on Industry, Research and Energy, Policy Department for Transformation, Innovation and Health, European Parliament; 2025, URL https://www.europarl.europa.eu/RegData/etudes/STUD/2025/772474/ECTI_STU(2025)772474_EN.pdf.

[10] Balasubramaniam BM, Thierry P-T, Lethier S, Pugnet V, Llewellyn P, Rajendran A. Process-performance of solid sorbents for Direct Air Capture (DAC) of CO_2 in optimized temperature-vacuum swing adsorption (TVSA) cycles. Chem Eng J 2024;485:149568. http://dx.doi.org/10.1016/j.cej.2024.149568, URL https://linkinghub.elsevier.com/retrieve/pii/S1385894724010532.

[11] Luukkonen A, Elfving J, Inkeri E. Improving adsorption-based direct air capture performance through operating parameter optimization. Chem Eng J 2023;471:144525. http://dx.doi.org/10.1016/j.cej.2023.144525, URL https://linkinghub.elsevier.com/retrieve/pii/S1385894723032564.

[12] Bouaboula H, Chaouki J, Belmabkhout Y, Zaabout A. Comparative review of direct air capture technologies: From technical, commercial, economic, and environmental aspects. Chem Eng J 2024;484:149411. http://dx.doi.org/10.1016/j.cej.2024.149411, URL https://linkinghub.elsevier.com/retrieve/pii/S1385894724008969.

[13] Terlouw T, Pokras D, Becattini V, Mazzotti M. Assessment of potential and techno-economic performance of solid sorbent direct air capture with CO_2 storage in Europe. Environ Sci Technol 2024;58(24):10567–81. http://dx.doi.org/10.1021/acs.est.3c10041, URL https://pubs.acs.org/doi/10.1021/acs.est.3c10041.

[14] Madhu K, Pauliuk S, Dhathri S, Creutzig F. Understanding environmental trade-offs and resource demand of direct air capture technologies through comparative life-cycle assessment. Nat Energy 2021;6(11):1035–44. http://dx.doi.org/10.1038/s41560-021-00922-6, URL https://www.nature.com/articles/s41560-021-00922-6.

[15] Heß D, Rubin M, Dittmeyer R. Carbon dioxide capture from air in buildings – Design and techno-economic feasibility of practical systems. J CO2 Util 2026;105:103351. http://dx.doi.org/10.1016/j.jcou.2026.103351, URL https://linkinghub.elsevier.com/retrieve/pii/S2212982026000405.

[16] Young J, McQueen N, Charalambous C, Foteinis S, Hawrot O, Ojeda M, et al. The cost of direct air capture and storage can be reduced via strategic deployment but is unlikely to fall below stated cost targets. One Earth 2023;6(7):899–917. http://dx.doi.org/10.1016/j.oneear.2023.06.004, URL https://linkinghub.elsevier.com/retrieve/pii/S2590332223003007.

[17] Keith DW, Holmes G, St. Angelo D, Heidel K. A process for capturing CO_2 from the atmosphere. Joule 2018;2(8):1573–94. http://dx.doi.org/10.1016/j.joule.2018.05.006, URL https://linkinghub.elsevier.com/retrieve/pii/S2542435118302253.

[18] Bisotti F, Hoff KA, Mathisen A, Hovland J. Direct air capture (DAC) deployment: A review of the industrial deployment. Chem Eng Sci 2024;283:119416. http://dx.doi.org/10.1016/j.ces.2023.119416, URL https://linkinghub.elsevier.com/retrieve/pii/S0009250923009727.

[19] Herzog H, Morris J, Gurgel A, Paltsev S. Getting real about capturing carbon from the air. One Earth 2024;7(9):1477–80. http://dx.doi.org/10.1016/j.oneear.2024.08.011, URL https://linkinghub.elsevier.com/retrieve/pii/S2590332224004214.

[20] Sievert K, Schmidt TS, Steffen B. Considering technology characteristics to project future costs of direct air capture. Joule 2024;8(4):979–99. http://dx.doi.org/10.1016/j.joule.2024.02.005, URL https://linkinghub.elsevier.com/retrieve/pii/S2542435124000606.

[21] An K, Li K, Yang C-M, Brechtl J, Nawaz K. A comprehensive review on regeneration strategies for direct air capture. J CO2 Util 2023;76:102587. http://dx.doi.org/10.1016/j.jcou.2023.102587, URL https://linkinghub.elsevier.com/retrieve/pii/S2212982023001981.

[22] Wijesiri RP, Knowles GP, Yeasmin H, Hoadley AFA, Chaffee AL. Technoeconomic evaluation of a process capturing CO_2 directly from air. Processes 2019;7(8):503. http://dx.doi.org/10.3390/pr7080503, URL https://www.mdpi.com/2227-9717/7/8/503.

[23] Fasihi M, Efimova O, Breyer C. Techno-economic assessment of CO_2 direct air capture plants. J Clean Prod 2019;224:957–80. http://dx.doi.org/10.1016/j.jclepro.2019.03.086, URL https://linkinghub.elsevier.com/retrieve/pii/S0959652619307772.

[24] Benkert S, Joos L, Wittstadt U, Will T, Burger A, Schnabel L, et al. High-temperature heat pump test bench with n-butane (R-600) generating steam. Chem Ing Tech 2026;98:364–73. http://dx.doi.org/10.1002/cite.70046, URL https://onlinelibrary.wiley.com/doi/abs/10.1002/cite.70046.

[25] Kosmadakis G, Arpagaus C, Neofytou P, Bertsch S. Techno-economic analysis of high-temperature heat pumps with low-global warming potential refrigerants for upgrading waste heat up to 150 °C. Energy Convers Manage 2020;226:113488. http://dx.doi.org/10.1016/j.enconman.2020.113488, URL https://linkinghub.elsevier.com/retrieve/pii/S0196890420310207.

[26] Burrin D, Roy S, Roskilly AP, Smallbone A. A combined heat and green hydrogen (CHH) generator integrated with a heat network. Energy Convers Manage 2021;246:114686. http://dx.doi.org/10.1016/j.enconman.2021.114686, URL https://linkinghub.elsevier.com/retrieve/pii/S0196890421008621.

[27] Van Der Roest E, Bol R, Fens T, Van Wijk A. Utilisation of waste heat from PEM electrolysers – Unlocking local optimisation. Int J Hydrog Energy 2023;48(72):27872–91. http://dx.doi.org/10.1016/j.ijhydene.2023.03.374, URL https://linkinghub.elsevier.com/retrieve/pii/S0360319923015410.

[28] Vázquez FV, Koponen J, Ruuskanen V, Bajamundi C, Kosonen A, Simell P, et al. Power-to-X technology using renewable electricity and carbon dioxide from ambient air: SOLETAIR proof-of-concept and improved process concept. J CO2 Util 2018;28:235–46. http://dx.doi.org/10.1016/j.jcou.2018.09.026, URL https://linkinghub.elsevier.com/retrieve/pii/S2212982018305213.

[29] Sendi M, Bui M, Mac Dowell N, Fennell P. Geospatial analysis of regional climate impacts to accelerate cost-efficient direct air capture deployment. One Earth 2022;5(10):1153–64. http://dx.doi.org/10.1016/j.oneear.2022.09.003, URL https://linkinghub.elsevier.com/retrieve/pii/S259033222200481X.

[30] Jajjawi AS, Wenzel H, Harzendorf F, Weinand JM, Stolten D, Peters R. Weather-dependent direct air capture process modeling for techno-economic assessments. Energy Convers Manage 2026;351:121003. http://dx.doi.org/10.1016/j.enconman.2025.121003, URL https://www.sciencedirect.com/science/article/pii/S0196890425015274.

[31] An K, Farooqui A, McCoy ST. The impact of climate on solvent-based direct air capture systems. Appl Energy 2022;325:119895. http://dx.doi.org/10.1016/j.apenergy.2022.119895, URL https://linkinghub.elsevier.com/retrieve/pii/S0306261922011588.

[32] Shorey P, Abdulla A. Liquid solvent direct air capture's cost and carbon dioxide removal vary with ambient environmental conditions. Commun Earth Environ 2024;5(1):607. http://dx.doi.org/10.1038/s43247-024-01773-1, URL https://www.nature.com/articles/s43247-024-01773-1.

[33] Wiegner JF, Grimm A, Weimann L, Gazzani M. Optimal design and operation of solid sorbent direct air capture processes at varying ambient conditions. Ind Eng Chem Res 2022;61(34):12649–67. http://dx.doi.org/10.1021/acs.iecr.2c00681, URL https://pubs.acs.org/doi/10.1021/acs.iecr.2c00681.

[34] Ge B, Zhang M, Hu B, Wu D, Zhu X, Eicker U, et al. Innovative process integrating high temperature heat pump and direct air capture. Appl Energy 2024;355:122229. http://dx.doi.org/10.1016/j.apenergy.2023.122229, URL https://linkinghub.elsevier.com/retrieve/pii/S0306261923015933.

[35] Wenzel H, Harzendorf F, Okosun K, Schöb T, Weinand JM, Stolten D. Weather conditions severely impact optimal direct air capture siting. Adv Appl Energy 2025;19:100229. http://dx.doi.org/10.1016/j.adapen.2025.100229, URL https://linkinghub.elsevier.com/retrieve/pii/S266679242500023X.

[36] Schellevis HM, De La Combé JD, Brilman DWF. Optimizing direct air capture under varying weather conditions. Energy Adv 2024;3(7):1678–87. http://dx.doi.org/10.1039/D4YA00200H, URL https://xlink.rsc.org/?DOI=D4YA00200H.

[37] Forman C, Muritala IK, Pardemann R, Meyer B. Estimating the global waste heat potential. Renew Sustain Energy Rev 2016;57:1568–79. http://dx.doi.org/10.1016/j.rser.2015.12.192, URL https://www.sciencedirect.com/science/article/pii/S1364032115015750.

[38] Luberti M, Gowans R, Finn P, Santori G. An estimate of the ultralow waste heat available in the European Union. Energy 2022;238:121967. http://dx.doi.org/10.1016/j.energy.2021.121967, URL https://linkinghub.elsevier.com/retrieve/pii/S0360544221022155.

[39] Mohan A, Konuru V, Luo H, Jenkins J. Direct air capture with thermal energy storage: process design and electricity system impacts. J Phys: Energy 2026;8(1):015011. http://dx.doi.org/10.1088/2515-7655/ae24ac, URL https://iopscience.iop.org/article/10.1088/2515-7655/ae24ac.

[40] Meriläinen A, Kosonen A, Jokisalo J, Kosonen R, Kauranen P, Ahola J. Techno-economic evaluation of waste heat recovery from an off-grid alkaline water electrolyzer plant and its application in a district heating network in Finland. Energy 2024;306:132181. http://dx.doi.org/10.1016/j.energy.2024.132181, URL https://linkinghub.elsevier.com/retrieve/pii/S0360544224019558.

[41] Meriläinen A, Jaatinen-Värri A, Uusitalo A, Kosonen A, Jokisalo J, Kosonen R, et al. Integration of water electrolysis and district heating through waste heat recovery in Nordic conditions: Techno-economic impacts of lowering the district heating network temperature. Energy 2026;344:139663. http://dx.doi.org/10.1016/j.energy.2025.139663, URL https://www.sciencedirect.com/science/article/pii/S0360544225053058.

[42] Ibáñez-Rioja A, Puranen P, Järvinen L, Kosonen A, Ruuskanen V, Hynynen K, et al. Baseload hydrogen supply from an off-grid solar PV–wind power–battery–water electrolyzer plant. Energy 2025;322:135304. http://dx.doi.org/10.1016/j.energy.2025.135304, URL https://linkinghub.elsevier.com/retrieve/pii/S0360544225009466.

[43] Ibáñez-Rioja A, Sakas G, Järvinen L, Puranen P. Off-grid green hydrogen production systems. In: Sguarezi Filho AJ, Jacomini RV, Capovilla CE, Casella IRS, editors. Smart grids–Renewable energy, power electronics, signal processing and communication systems applications. Cham: Springer International Publishing; 2024, p. 37–72. http://dx.doi.org/10.1007/978-3-031-37909-3_2.

[44] El-Shafie M. Hydrogen production by water electrolysis technologies: A review. Results Eng 2023;20:101426. http://dx.doi.org/10.1016/j.rineng.2023.101426, URL https://linkinghub.elsevier.com/retrieve/pii/S2590123023005534.

[45] Fabiani T, Le Pierrès N, Tochon P, Dumoulin P. Thermal management of solid oxide electrolysis cell systems: Integration principles, coupling with external heat sources and integration of heat storage technologies. Appl Energy 2025;401:126539. http://dx.doi.org/10.1016/j.apenergy.2025.126539, URL https://linkinghub.elsevier.com/retrieve/pii/S0306261925012693.

[46] Ibáñez-Rioja A, Puranen P, Järvinen L, Kosonen A, Ruuskanen V, Ahola J, et al. Simulation methodology for an off-grid solar-battery-water electrolyzer plant: Simultaneous optimization of component capacities and system control. Appl Energy 2022;307:118157. http://dx.doi.org/10.1016/j.apenergy.2021.118157, URL https://www.sciencedirect.com/science/article/pii/S0306261921014306.

[47] Ibáñez-Rioja A, Järvinen L, Puranen P, Kosonen A, Ruuskanen V, Hynynen K, et al. Off-grid solar PV-wind power-battery-water electrolyzer plant: Simultaneous optimization of component capacities and system control. Appl Energy 2023;345:121277. http://dx.doi.org/10.1016/j.apenergy.2023.121277, URL https://linkinghub.elsevier.com/retrieve/pii/S0306261923006414.

[48] Luukkonen A, Elfving J. Optimizing direct air capture: evaluating the impact of process parameters on productivity, energy requirement, and cost. In: Proceedings of the 17th greenhouse gas control technologies conference. GHGT-17, Calgary, Canada; 2024, http://dx.doi.org/10.2139/ssrn.5014185.

[49] Wang W, Zhang Y, Liu W, Wang T, Fang M, Zhang X, et al. Temperature vacuum swing adsorption for post-combustion carbon capture with different process configurations. Energy 2025;334:137520. http://dx.doi.org/10.1016/j.energy.2025.137520, URL https://linkinghub.elsevier.com/retrieve/pii/S0360544225031627.

[50] Joss L, Gazzani M, Mazzotti M. Rational design of temperature swing adsorption cycles for post-combustion CO_2 capture. Chem Eng Sci 2017;158:381–94. http://dx.doi.org/10.1016/j.ces.2016.10.013, URL https://www.sciencedirect.com/science/article/pii/S0009250916305425.

[51] Holmes HE, Kim J, Realff MJ. Process systems engineering: a key enabler of adsorption-based direct air capture. Curr Opin Chem Eng 2026;51:101202. http://dx.doi.org/10.1016/j.coche.2025.101202, URL https://linkinghub.elsevier.com/retrieve/pii/S2211339825001145.

[52] Rezo D, Glaser M, Postweiler P, Engelpracht M, von der Assen N. Control strategies to optimize adsorption-based direct air capture under varying weather conditions. Appl Energy 2026;411:127578. http://dx.doi.org/10.1016/j.apenergy.2026.127578, URL https://www.sciencedirect.com/science/article/pii/S0306261926002308.

[53] Schellevis HM, Brilman DWF. Experimental study of CO_2 capture from air *via* steam-assisted temperature-vacuum swing adsorption with a compact kg-scale pilot unit. React Chem Eng 2024;9(4):910–24. http://dx.doi.org/10.1039/D3RE00460K, URL https://xlink.rsc.org/?DOI=D3RE00460K.

[54] Lilonfe S, Rodgers S, Abdul-Manan AF, Dimitriou I, McKechnie J. Technical, economic and lifecycle greenhouse gas emissions analyses of solid sorbent direct air capture technologies. Carbon Capture Sci Technol 2025;15:100380. http://dx.doi.org/10.1016/j.ccst.2025.100380, URL https://linkinghub.elsevier.com/retrieve/pii/S277265682500020X.

[55] Bos M, Kersten S, Brilman D. Wind power to methanol: Renewable methanol production using electricity, electrolysis of water and CO_2 air capture. Appl Energy 2020;264:114672. http://dx.doi.org/10.1016/j.apenergy.2020.114672, URL https://linkinghub.elsevier.com/retrieve/pii/S0306261920301847.

[56] Grimm A, Kramer GJ, Gazzani M. How would ideal sorbents improve the technical and economic performance of adsorption-based direct air capture? Energy Fuels 2024;38(19):18781–99. http://dx.doi.org/10.1021/acs.energyfuels.4c01156, URL https://pubs.acs.org/doi/10.1021/acs.energyfuels.4c01156.

[57] National Academies of Sciences, Engineering, and Medicine. Negative emissions technologies and reliable sequestration: a research agenda. Tech. rep., Washington, D.C.: The National Academies Press; 2019, http://dx.doi.org/10.17226/25259, URL https://www.nationalacademies.org/publications/25259.

[58] Schmidt T, Pauschinger T, Sørensen PA, Snijders A, Djebbar R, Boulter R, et al. Design aspects for large-scale pit and aquifer thermal energy storage for district heating and cooling. Energy Procedia 2018;149:585–94. http://dx.doi.org/10.1016/j.egypro.2018.08.223, URL https://linkinghub.elsevier.com/retrieve/pii/S1876610218305198.

[59] Danish Energy Agency, Energinet. Technology data – Energy storage. Tech. rep., Danish Energy Agency; 2018, URL https://ens.dk/en/our-services/projections-and-models/technology-data/technology-data-energy-storage.

[60] Østergaard PA, Andersen AN. Optimal heat storage in district energy plants with heat pumps and electrolysers. Energy 2023;275:127423. http://dx.doi.org/10.1016/j.energy.2023.127423, URL https://www.sciencedirect.com/science/article/pii/S0360544223008174.

[61] Grosse R, Christopher B, Stefan W, Geyer R, Robbi S. Long term (2050) projections of techno-economic performance of large-scale heating and cooling in the EU. Tech. rep., Luxembourg: Publications Office of the European Union; 2017, URL https://data.europa.eu/doi/10.2760/24422.

[62] Climeworks. Orca: the first large-scale plant. 2026, URL https://climeworks.com/plant-orca [Accessed 19 March 2026].

[63] Smith E, Morris J, Kheshgi H, Teletzke G, Herzog H, Paltsev S. The cost of CO_2 transport and storage in global integrated assessment modeling. Int J Greenh Gas Control 2021;109:103367. http://dx.doi.org/10.1016/j.ijggc.2021.103367, URL https://linkinghub.elsevier.com/retrieve/pii/S1750583621001195.

[64] Climeworks. Next generation tech powers Climeworks' megaton leap. 2026, URL https://climeworks.com/press-release/next-gen-tech-powers-climeworks-megaton-leap [Accessed 10 March 2026].
[65] Paajanen A, Nevaranta N, Bajamundi C. Modeling and control of heating and heat circulation in direct air capture system. Chem Eng Sci 2025;301:120745. http://dx.doi.org/10.1016/j.ces.2024.120745, URL https://www.sciencedirect.com/science/article/pii/S0009250924010455.
[66] Holmes HE, Banerjee S, Vallace A, Lively RP, Jones CW, Realff MJ. Tuning sorbent properties to reduce the cost of direct air capture. Energy Environ Sci 2024;17(13):4544–59. http://dx.doi.org/10.1039/D4EE00616J, URL https://pubs.rsc.org/en/content/articlelanding/2024/ee/d4ee00616j.
[67] Chauvy R, Dubois L, Lybaert P, Thomas D, De Weireld G. Production of synthetic natural gas from industrial carbon dioxide. Appl Energy 2020;260:114249. http://dx.doi.org/10.1016/j.apenergy.2019.114249, URL https://linkinghub.elsevier.com/retrieve/pii/S0306261919319361.
[68] Sollai S, Porcu A, Tola V, Ferrara F, Pettinau A. Renewable methanol production from green hydrogen and captured CO_2: A techno-economic assessment. J CO2 Util 2023;68:102345. http://dx.doi.org/10.1016/j.jcou.2022.102345, URL https://linkinghub.elsevier.com/retrieve/pii/S2212982022004644.
[69] Xiang Y, Xie Z, Furbo S, Wang D, Gao M, Fan J. A comprehensive review on pit thermal energy storage: Technical elements, numerical approaches and recent applications. J Energy Storage 2022;55:105716. http://dx.doi.org/10.1016/j.est.2022.105716, URL https://www.sciencedirect.com/science/article/pii/S2352152X22017042.
[70] Lieskoski S, Koskinen O, Tuuf J, Björklund-Sänkiaho M. A review of the current status of energy storage in Finland and future development prospects. J Energy Storage 2024;93:112327. http://dx.doi.org/10.1016/j.est.2024.112327, URL https://linkinghub.elsevier.com/retrieve/pii/S2352152X24019133.
[71] Bamigbetan O, Eikevik TM, Nekså P, Bantle M, Schlemminger C. Experimental investigation of a prototype R-600 compressor for high temperature heat pump. Energy 2019;169:730–8. http://dx.doi.org/10.1016/j.energy.2018.12.020, URL https://linkinghub.elsevier.com/retrieve/pii/S0360544218323867.
[72] Verdnik M, Rieberer R. Influence of operating parameters on the COP of an R600 high-temperature heat pump. Int J Refrig 2022;140:103–11. http://dx.doi.org/10.1016/j.ijrefrig.2022.05.010, URL https://www.sciencedirect.com/science/article/pii/S0140700722001621.
[73] Bell IH, Wronski J, Quoilin S, Lemort V. Pure and pseudo-pure fluid thermophysical property evaluation and the open-source thermophysical property library CoolProp. Ind Eng Chem Res 2014;53(6):2498–508. http://dx.doi.org/10.1021/ie4033999.
[74] El Samad T, Żabnieńska-Góra A, Jouhara H, Sayma AI. A review of compressors for high temperature heat pumps. Therm Sci Eng Prog 2024;51:102603. http://dx.doi.org/10.1016/j.tsep.2024.102603, URL https://linkinghub.elsevier.com/retrieve/pii/S245190492400221X.
[75] Brown RN. Compressors: Selection and sizing. 3rd ed.. Amsterdam ; Boston: Elsevier; 2005.
[76] Ma Y, He Z, Peng X, Xing Z. Experimental investigation of the discharge valve dynamics in a reciprocating compressor for trans-critical CO_2 refrigeration cycle. Appl Therm Eng 2012;32:13–21. http://dx.doi.org/10.1016/j.applthermaleng.2011.03.022, URL https://linkinghub.elsevier.com/retrieve/pii/S1359431111001542.
[77] Bai Y, Yang M, Fan J, Li X, Chen L, Yuan G, et al. Influence of geometry on the thermal performance of water pit seasonal heat storages for solar district heating. Build Simul 2021;14(3):579–99. http://dx.doi.org/10.1007/s12273-020-0671-9.
[78] Schütz T, Harb H, Streblow R, Müller D. Comparison of models for thermal energy storage units and heat pumps in mixed integer linear programming. In: 28th international conference on efficiency, cost, optimization, simulation and environmental impact of energy systems. ECOS, Pau, France; 2015.
[79] He M, Wang Z, Zhang J, Yuan G, Yang J, Yang M, et al. Study on heat transfer process of insulated floating cover of water pit for solar seasonal thermal storage. Energy Rep 2022;8:1396–404. http://dx.doi.org/10.1016/j.egyr.2022.09.060, URL https://www.sciencedirect.com/science/article/pii/S235248472201784X.
[80] Fan J, Huang J, Chatzidiakos A, Furbo S. Experimental and theoretic investigations of thermal behavior of a seasonal water pit heat storage. In: Proceedings of SWC2017/SHC2017. Abu Dhabi: International Solar Energy Society; 2017, p. 1–12. http://dx.doi.org/10.18086/swc.2017.13.03, URL http://proceedings.ises.org/citation?doi=swc.2017.13.03.
[81] Yli-Halla M, Mokma D. Soil temperature regimes in Finland. Agric Food Sci 1998;7(4):507–12. http://dx.doi.org/10.23986/afsci.5606, URL https://journal.fi/afs/article/view/5606.
[82] Lemmelä R, Sucksdorff Y. Annual variation of soil temperature at depth 20 to 700 cm in an experimental field in Hyrylä, South-Finland during 1969 to 1973. Geophysica 1981;17:143–54, URL https://www.geophysica.fi/pdf/geophysica_1981_17_1-2_143_lemmela.pdf.
[83] Nord Pool. Day-ahead prices. 2024, URL https://data.nordpoolgroup.com/auction/day-ahead/prices?deliveryDate=latest&currency=EUR&aggregation=DeliveryPeriod&deliveryAreas=FI [Accessed 26 November 2024].
[84] Statistics Finland. Energy prices – Price of electricity by type of consumer. 2024, URL https://pxdata.stat.fi/PxWeb/pxweb/en/StatFin/StatFin_ehi/statfin_ehi_pxt_13rb.px/ [Accessed 26 November 2024].
[85] Finnish Energy. Energy year 2025 - Electricity. 2026, URL https://energia.fi/en/statistics/statistics-on-electricity/ [Accessed 15 June 2026].
[86] Pieper H, Ommen T, Buhler F, Paaske BL, Elmegaard B, Markussen WB. Allocation of investment costs for large-scale heat pumps supplying district heating. Energy Procedia 2018;147:358–67. http://dx.doi.org/10.1016/j.egypro.2018.07.104, URL https://linkinghub.elsevier.com/retrieve/pii/S1876610218302613.
[87] Danish Energy Agency, Energinet. Technology data – Generation of electricity and district heating, data sheets version 0019. Tech. rep., Danish Energy Agency; 2026, URL https://ens.dk/en/analyses-and-statistics/technology-data-generation-electricity-and-district-heating.
[88] Vocale P, Morini GL, Spiga M. Influence of outdoor air conditions on the air source heat pumps performance. Energy Procedia 2014;45:653–62. http://dx.doi.org/10.1016/j.egypro.2014.01.070, URL https://www.sciencedirect.com/science/article/pii/S187661021400071X.
[89] Rossi di Schio E, Ballerini V, Dongellini M, Valdiserri P. Defrosting of air-source heat pumps: Effect of real temperature data on seasonal energy performance for different locations in Italy. Appl Sci 2021;11(17):8003. http://dx.doi.org/10.3390/app11178003, URL https://www.mdpi.com/2076-3417/11/17/8003.
[90] Kropas T, Streckienė G, Bielskus J. Experimental investigation of frost formation influence on an air source heat pump evaporator. Energies 2021;14(18):5737. http://dx.doi.org/10.3390/en14185737, URL https://www.mdpi.com/1996-1073/14/18/5737.